July 31, 2015

South Dakota School of Mines and Technology

Shale Research Initiative - Final Report

Executive Summary

The State of South Dakota allotted $464,000 to the SD Board of Regents during FY2014 to conduct research in shale in South Dakota. The South Dakota School of Mines and Technology (SDSM&T) used these funds to investigate portions of the Pierre Shale Group and Niobrara Formation to determine the properties of these units in the deeper subsurface. Although the main thrust of the research was to develop a better understanding of the geomechanical behavior of the Pierre Shale, this unit and the underlying Niobrara Formation are of particular interest because of their potential for hydrocarbon development in some areas of western South Dakota. In order to acquire samples for geomechanical testing and other investigations, a coring program was undertaken that acquired continuous core below the zone of weathering. The success of the initial coring program northwest of Ft. Pierre, SD, and the recognition that important scientific objectives could be achieved as a complementary effort led the Department of Natural Resources-South Dakota Geological Survey (DENR-SDGS) to join the project. This greatly expanded the reach of the originally conceived research. As a result, an additional three holes were drilled in the vicinity of Presho, SD, two of which were continuously cored with excellent core quality and recovery. The participation of the DENR-SDGS significantly enhanced the current and future effects of this project. The availability of core from these important geologic units attracted the interest of the Department of Energy-National Engineering Technology Laboratory (DOE-NETL), which has committed to performing scanning of the cores using a variety of non-invasive techniques. Other work will include performance of source rock analysis for hydrocarbon potential at selected intervals along the cores. These collaborations resulted in the formation of an excellent, multi-faceted team involving state and federal agencies, as well as South Dakota industry that will continue into the future using the materials acquired during the project.

This report summarizes the work that was conducted during the course of the project, but will only touch briefly upon some of the results that have been derived to date. Examples in the attached appendices illustrate the variety of investigations undertaken including preliminary geomechanical work, computer tomography, stratigraphic and paleontological studies, and oil/gas shows encountered. Future work will include further delineation of the hydrocarbon system in the Pierre Shale and Niobrara Formation, applications for appropriate funding from federal and private sources for geomechanical work on the shales, and stratigraphic studies linking South Dakota units to other regional geologic units.

Contents

1. Introduction

The South Dakota School of Mines & Technology (SDSM&T) has a long-standing interest in shales and other fine-grained geologic media. For example, the team of SDSM&T and RESPEC, a Rapid City-based engineering firm, were funded in 2012 by the Department of Energy (DOE) Used Nuclear Fuel Disposition program to investigate generic, non-site-specific issues associated with potential nuclear waste disposal in shale and other fine-grained geologic materials. Shale is a fine-grained, detrital sedimentary rock formed by the consolidation of clay, silt, or mud. This rock type is one of the most common geologic units in South Dakota and the surrounding region, both at the surface and in the subsurface. Although shale comprises much of the surficial cover in western South Dakota and often extends to depths of thousands of feet, these units are well represented in the subsurface of eastern South Dakota, as well. The State of South Dakota allotted $464,000 to the SD Board of Regents during FY2014 to conduct research in shale in South Dakota. The South Dakota School of Mines and Technology used these funds to investigate portions of the Pierre Shale and Niobrara Formation for the purpose of determining the properties of these units in the deeper subsurface.

2. Mission of the Initiative

The development of a shale research initiative at SDSM&T is intended to provide a mechanism for the university, along with its industrial and governmental partners, to lead research in the field of shale geoscience and geoengineering. With the recent funding provided by the state of South Dakota, the research team is contributing significantly to the state of knowledge and to developing a foundation of research that includes investigating the properties, mineralogy, composition, and uses of various shale units. Ongoing research that began with this project will be applicable for multiple industries where the understanding of the behavior of shale and other fine-grained geological units is critical.

3. Scope of this Report

The project funding was limited to one South Dakota fiscal year that ended June 30, 2015. Therefore, it proved to be challenging to develop a plan, execute the plan for sample acquisition, perform initial analyses, establish collaborations, and consider future research needs within that time frame. Great strides were made toward accomplishing these goals, and important preliminary data were acquired regarding the resources, scientific and otherwise, within the shales of western South Dakota. Investigations began during the project are expected to continue, which will ensure the efficient use of the funding. Given these considerations, this report is limited primarily to descriptions of work done on the project, which primarily involved drilling and coring within the shale bedrock. Brief summations of some results to date are included as appendices in this report. Results from the final analyses will be reported later in the scientific literature either in cooperation with the collaborating agencies or as stand-alone documents.

4. Tasks

This report is organized along the lines of the Letter of Intent submitted to the South Dakota Board of Regents at the beginning of the project in 2014. That document described the activities that would be conducted during the project, along with the expected benefits. The following tasks are similar to those of the Letter of Intent, although they have been rearranged somewhat to provide a more logical flow for the tasks along a timeline.

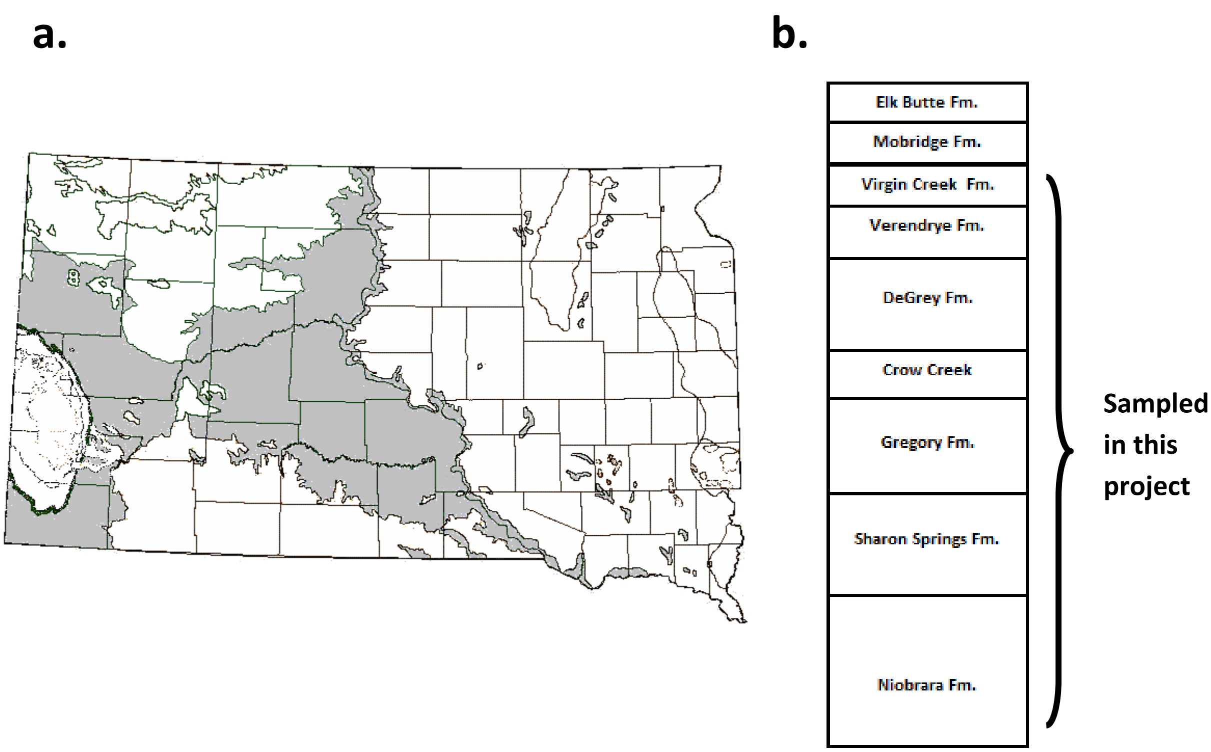

Figure 4-1 a. Outcrop of area of the Upper Cretaceous shales in South Dakota (from DENR-SDGS simplified geologic map of South Dakota). b. The stratigraphic section of the section penetrated in this investigation is shown to the right in the diagram.

4.1 Task I Sample Acquisition and Description of the Coring Operations

Figure 4-1 shows the outcrop area of the Pierre Shale in South Dakota along with the portion of the stratigraphic section penetrated by the drilling operations. The widespread distribution of shale in South Dakota, both in outcrop (horizontal distribution) and stratigraphically (vertical/thickness distribution) reflects its potential importance to the State of South Dakota. The characteristics of the surficial occurrences of these shales are very different from properties in the deeper subsurface, however. Whereas the geotechnical and geochemical nature of the Pierre Shale at the surface is well understood through decades of research driven by transportation needs and dam construction, the unaltered subsurface shale can reasonably be considered a different material. Very often when shale is exposed to the weathering effects at the surface, along with fresh water through rain or water impoundment, the subsurface rock quickly loses cohesion and crumbles into flakes, eventually becoming soil. Rewetting of the degraded shale results in the "gumbo" encountered across much of the state.

The rapid degradation of the Pierre Shale at the surface requires drilling and coring to retrieve intact samples from the subsurface. These intact samples then can be specially preserved and subjected to analysis for deformational properties and structures that otherwise would be destroyed by the processes undergone at the surface. As a result of these considerations, the current project focused on recovery of material from the subsurface through drilling and coring.

The scope of the project expanded through the collaboration with the DENR-SDGS. As a result, a greater amount of core will be available for future research. The recovered cores will not only provide answers to questions in the short term but will also be a long term resource housed at the DENR-SDGS core archive facility in Vermillion, SD. This will ensure that future researchers will be able to access these materials.

4.1.1 Tree Dam

Beginning in July 2014, drilling operations commenced in an open area at the Triple U Buffalo Ranch approximately 27 miles northwest of Pierre, SD, as shown in Figure 4-2. The drill hole was known as the Tree Dam Hole, and a total depth (TD) of 512 feet (ft.) was achieved before drilling had to be curtailed because of drilling problems associated with slough falling into the uncased hole from unconsolidated sand in the Crow Creek Member of the Pierre Shale approximately 58 ft above the TD. The hole was drilled and cored by Major Drilling, Inc., a private contractor. The advancement rate was excellent with good core recovery and quality. In order to ensure mechanical stability, the core was placed in approximately 5 ft long PVC pipe. One half of the cores were wrapped in cling film and one half was preserved in mineral oil and the ends of the pipe sealed. The cling film wrapped material is being evaluated for hydrocarbon content, which would not be possible if preserved in mineral oil. The mineral oil cores are preserved in this manner to ensure geomechanical and geochemical stability in anticipation of geomechanical testing. This type of preservation is commonly used to ensure that shale cores can be stored for longer periods of time without degradation associated with changes in moisture.

Figure 4-2. Location of drilling. The Tree Dam location is northwest of Pierre, SD. The three Presho holes are located near Presho, SD: Presho #1 is located 11 miles south of Presho, and Presho #2 and test hole M51-2015-2 are located 1.5 miles southeast of Presho, SD.

4.1.2 Presho #1

Coring operations by the DENR-SDGS began in September, 2014, and continued into December. The location of this hole was 11 miles south of Presho, SD, (Figs. 4-2 and 4-3) and had a goal of coring the lower Pierre Shale and the underlying Niobrara Formation. Core quality and recovery was excellent and a total of 554 ft were drilled in this location. Although the entire Pierre Shale section was not penetrated, drilling operations were suspended in December 2014, because of the onset of winter.

Figure 4-3. Location of Presho #1 and Presho #2.

4.1.3 Presho #2

Because the entire lower Pierre Shale had not been penetrated and the Niobrara Formation had not been reached, drilling operations at Presho resumed in April 2015, at a location approximately 1.5 miles southeast of Presho, SD (test hole R20-2015-12). The top of this hole was approximately 50 ft. higher than the bottom of Presho #1, which ensured overlap so that no stratigraphy in the lower Pierre Shale would be missed. This hole was plugged after a total depth of 628 ft. was reached. This depth, along with Presho #1, sampled a complete section of the lower Pierre Shale and a probable penetration of the Niobrara Formation. In addition to the description of the cores at the drill site as a geologic log, electric logs were run whenever possible. These data will allow correlations to be made with wells and test holes in the local area, as well as in the region.

4.1.4 Test Hole M51-2015-2

Test hole M51-2015-2 was drilled about 75 ft. to the northeast from Presho #2. This hole is known as test hole R20-2015-12 by the DENR-SDGS, and it was drilled for electric logging purposes. Difficulties with the hole limited the total depth and an abbreviated electric log was acquired.

4.2 Task II Coordination with Federal, State, and Local Agencies

One of the major goals of the project was to develop collaborations among interested agencies and institutions, and efforts in that direction were successful on several levels. The cooperation of the DENR-SDGS was paramount to the success of the drilling projects. Originally, the drilling was envisioned to be confined to the Tree Dam (Pierre) hole, but it was recognized that the addition of another coring opportunity would benefit the scientific and economic goals of South Dakota and the project. The DENR-SDGS contributed all of the drilling near Presho, SD. The coring locations south of Presho, SD, also offered the possibility of drilling into and through the Niobrara Formation. This meshed well with an ongoing project funded by the American Indian Higher Education Consortium. This project is investigating the potential of the Niobrara Formation for small-scale gas production (refer to Appendix G). Combining these parallel and complimentary goals into one project leveraged the results tremendously. After completion of the current testing programs, all of the cores acquired in this project will be under the care of the DENR-SDGS at the core archive facility in Vermillion, SD. Therefore, they will constitute a well-conserved resource for further research on this important part of South Dakota history.

Joint agency analysis of the cores was performed in the field through core descriptions, and more detailed work will be performed now that the core acquisition phase has been completed. Post-field description core scanning was conducted on one-half of the Tree Dam core at the Morgantown, WV, facility of the Department of Energy National Engineering Technology (DOE-NETL), and nearly all of the Presho cores were shipped in June, 2015, for similar scanning. The scanning of the core involves photography and closely spaced measurement of magnetic susceptibility, density, electrical conductivity, acoustic P-wave velocity, rock composition using X-ray fluorescence, and natural gamma radiation. Source analyses for hydrocarbon generation already have been performed on the Tree Dam material, and the Presho cores will be similarly sampled with special attention being given to the Niobrara Formation samples. A Memorandum of Understanding (MOU) will be signed between SDSM&T, DENR-South Dakota Geological Survey, and DOE-NETL. This MOU describes the protocol for the handling of the cores and samples, and establishes protocols for subsequent publications resulting from the work on this project.

Although no formal agreements are in place, Sandia National Laboratories has performed some preliminary work on a system for the extraction of pore water from the shale. Preliminary scoping indicates that the system is capable of extraction of such water. As a result, personnel from Sandia have participated in one proposal as a cooperator with SDSM&T. Although that proposal was not successful, it is anticipated that efforts will be undertaken in the future with additional submissions.

4.3 Task III Advanced Laboratory Testing

Testing for geomechanical properties of the shale was performed at the laboratories of RESPEC, Inc. and SDSM&T, both of which are located in Rapid City, SD. Although a variety of geomechanical tests were run, some of the most novel and interesting tests investigated the creep properties of the shale. Creep deformation is a time dependent process which is best evaluated when the stress difference on the shale sample is held constant. In some circumstances, the continuing creep deformation results in failure of the sample after some duration of time, even though the stress difference is unchanged. This failure mechanism is a major, controlling parameter in the geomechanical behavior of shale, but is currently poorly understood. Appendix A, Geomechanical Laboratory Analyses, describes the work performed as this part of the task. This work constituted a major portion of the analytical research, and preliminary results already indicate significant progress. Appendix B, Description of New Triaxial Testing Machine describes a new piece of equipment that is especially useful for working with the shale samples acquired during this project.

Other analytical work performed at SDSM&T included CT (computer tomography) and scanning electron microscopy (SEM) that is described in Appendix C, which allowed the small-scale morphologies of samples to be imaged. Appendix D includes a discussion of the Crow Creek Member, a thin unit that my have formed as a result of the Manson Meteor Impact in northwestern Iowa at approximately 75 million years ago. An investigation of the micropaleontologic fauna from Presho #1 is included as Appendix E. Other studies included stratigraphic relationships based upon regional correlations with the drilled sequences. This type of analysis was completed in order to delineate potential hydrocarbon source rocks and potential reservoir within the Niobrara Formation. It also will provide a basis from which to correlate and compare hydrocarbon-producing strata in areas such as Wyoming and Colorado with similar strata in South Dakota.

4.4 Task IV Task Energy Development - Economic Development

The project already has produced significant economic implications. As described in previous sections, the development of a collaboration between DOE-NETL and the other members of the project advanced the project substantially. This is further described in a recent article in the American Association of Petroleum Geologists Explorer entitled, “Assessing Potential of the Rosebud Reservation”, included as Appendix G. It was noted that a funded project involving a collaboration of Sinte Gleska University, SDSM&T, and DOE-NETL has been in place since 2012. The project involves Native American students in the assessment of whether it is feasible to use natural gas from the Niobrara Formation as a possible low-volume, shallow depth energy source. The current project acquired samples of the Niobrara Formation near the Rosebud Reservation, and analysis of the potential of this material to generate oil and gas will provide information for the direct evaluation of that resource.

4.4.1 Tree Dam (near Ft. Pierre, SD) and Presho #2

An oil show from the Tree Dam core was encountered at a depth of 202 feet Examination of the core showed a small, two-foot section where the film originated (Fig. 4-4 a.). The small amount of hydrocarbon, shallow depth, and impermeability of the shale indicates that the show would not be commercially productive, but it is of interest, nonetheless. Source rock analysis of this portion of the sample at the laboratory of the DOE-NETL found an elevated amount of kerogen (Type III) in the vicinity of the show.

Although Presho #1 did not have any hydrocarbon shows, the Presho #2 test hole had frequent evidence of fluids that appeared to be either oily or gaseous (Fig. 4-4 b.). In no instances, was there evidence that the shows might represent commercial accumulations, but they are of interest in understanding possible hydrocarbon systems in the region, such as identifying hydrocarbon source rocks and hydrocarbon migration pathways. The cores from this hole will be undergoing source rock analysis measurements to gain a better idea of source rock potential. The oil and gas shows encountered during the coring for the Tree Dam Hole and Presho #2 are listed in Appendix F.

a.

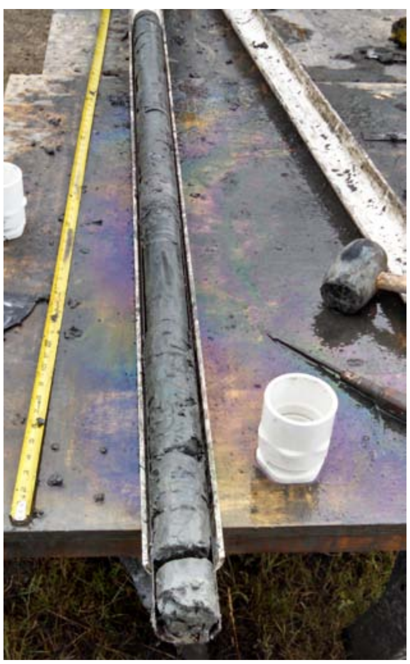

b.

Figure 4-4. **a.** Light oil show from the Tree Dam core at approximately 202 ft. depth. **b.** Good oil show from Presho #2 at about 585 ft. depth (picture credit DENR-SDGS).

4.5 Task VI Future Research Plan

This project has laid the foundation for a wide variety of future research directions. The analyses of hydrocarbon potential from the lower Pierre Shale and Niobrara Formation should provide excellent information that can support ongoing projects for hydrocarbon development as described in Appendix G. The gas shows in the Niobrara Formation in western South Dakota have been a long-standing topic of speculation, and source rock analyses from this project along with the currently funded project in Appendix G will provide much information to help resolve some of these uncertainties.

Subsequent proposals using the materials, methods, and results from the current project are anticipated. This includes follow on work regarding the geomechanical behavior of the shale, which is important for storage applications, as well as providing important insights on the fundamental process by which shales deform over time. Numerous venues for the future proposals are available, although the Department of Energy probably is the most obvious opportunity through their yearly call for proposal process. Other likely projects include investigations of the composition of the pore water in the shale. Samples acquired for this purpose during the coring process were preserved in paraffin wax to ensure that air could not alter the geochemistry of the fluids trapped in the shale and also to ensure that water could not escape. Considerable interest in this type of investigation has been shown by the Department of Energy and a preliminary extraction apparatus has been assembled for this purpose at one of the national laboratories. This preliminary work on samples acquired during this project show that it is possible to squeeze the shale sufficiently to force water from the dispersed porosity within the shale.

It was anticipated that future funding would be acquired from the petroleum industry whose interest might primarily be related to the development of better understanding of the deformation processes of the shale. The well-documented, sudden downturn of the petroleum industry within the past year has made it difficult to develop those industry connections and interest. Nevertheless, the results of the current investigations will prove useful to the industry, and as the commodity cycle continues, interest from industry may be revived.

A major task within any scientific and engineering investigation is the requirement to disseminate the results of the work. This project is no different in that regard, and it is anticipated that a number of journal publications will be prepared based upon the work of the past year as well as the follow-on work. In addition to possible scientific publications, one or more dedicated sessions at scientific conferences are being investigated as possibilities for focused meetings that would bring an even wider range of investigators together to consider problems associated with the Pierre Shale and the underlying Niobrara Formation.

5. Budget Notes and Explanations

The expenses and work on this project were directed toward acquisition, preservation, and analysis of the materials from the subsurface of the Pierre Shale. A graphical depiction of the general budget categories is shown in Figure 5-1 and listed in Table 5-1. A brief description of the items in each of the budget categories is presented in the following sections.

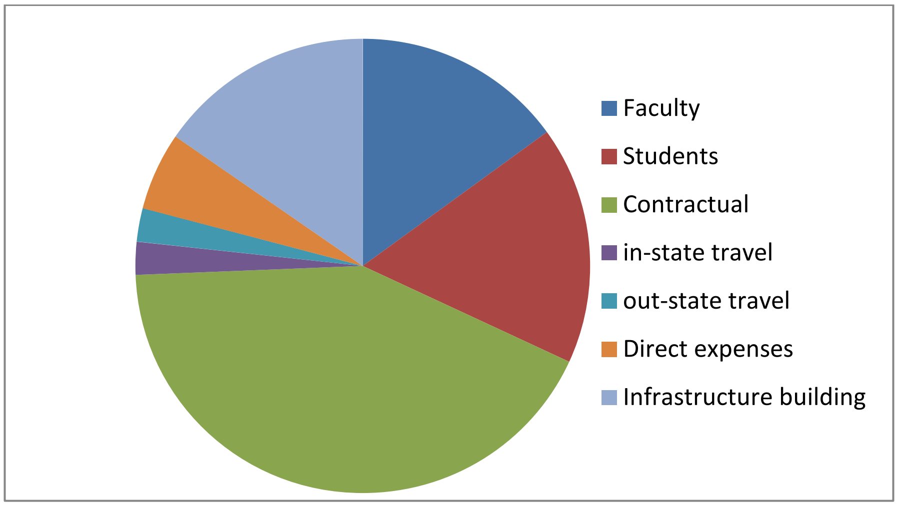

Figure 5-1. Distribution of Expenditures on the Project in Terms of General Categories

Table 5-1. Percentages and Amounts for Each General Category of Expenditures

	%	Amount
Faculty	15.0	$ 69,528
Students	16.9	$ 78,576
Contractual	42.4	$ 196,948
in-state travel	2.3	$ 10,893
out-state travel	2.4	$ 11,009
Direct expenses	5.5	$ 25,746
Infrastructure building	15.4	$ 71,300

5.1 Faculty

The faculty and staff funded on this project are members of the Department of Geology and Geological Engineering and the Department of Mining Engineering and Management with the South Dakota School of Mines and Technology. The activities included work on geomechanics of the shale, computer tomography, student oversight, in-field support of drilling, and project management.

5.2 Students

A total of eight students were funded at various levels for their work on this project. These included two undergraduates who were involved in the coring operation (one from the Department of Mining and Engineering Management and one from the Department of Mechanical Engineering). Six graduate students participated in the investigations, who are working on degrees in the Department of Geology and Geological Engineering and the Department of Mining Engineering and Management (one Ph.D. student and five M.S. students). The graduate students worked on stratigraphic analyses, geomechanical behavior of the shale samples, and computer tomography (CT) that examined the internal structure of the shale.

5.3 Contractual Services

The two types of contractual services used included costs for drilling and coring the hole northwest of Pierre, SD, known as the Tree Dam Hole and expenses incurred through RESPEC, Inc. for geomechanical analysis and testing of deformation. Of these expenses, $150,000 was allocated to RESPEC for advanced laboratory testing, numerical modeling, and project management and the remainder of the contractual serves was paid to Major Drilling Company for drilling the Tree Dam Hole (See Table 5-1 and Figure 5-1).

5.4 Travel

5.4.1 In-State Travel

Travel within South Dakota fell into two general categories, including travel in support of the drilling activities and travel to make presentations at in-state meetings. The bulk of this type of travel was used to keep a person at the drill site to assist in the coring activities, which included preservation and documentation of the subsurface samples. This required trips each week to the coring site(s) plus related lodging costs. Several presentations at engineering, science, and budgetary meetings also were held within the state. As can be seen in Table 5-1 and Figure 5-1, in-state costs amounted to approximately one-half of the total travel costs.

5.4.2 Out-of-State Travel

Out-of-State travel consisted of expenses associated with a workshop aimed at understanding the use of computer tomography, a presentation of results at a professional meeting, and expenses associated with core analysis. Portions of the core from the first hole were transported to the DOE-NETL facility in Morgantown, WV, to perform whole core analysis. This trip amounted to nearly one-half of the out-of-state expenses with the remainder being allocated to the other trips mentioned previously.

5.5 Direct Expenses

Materials to characterize and preserve the samples as well as to assist in their analysis are included within this general category. Examples of these types of costs include mineral oil for preservation of one-half of the Tree Dam core to minimize geochemical reactions during storage, PVC pipe for mechanical stability of the shale cores and core storage, equipment for the separation of microfossils from the end pieces of individual core runs, and the replacement of damaged drill steel. Many other miscellaneous items, none in excess of $1,000, were necessary to conduct the research. Overall, the direct expenses added up to approximately 5.5 percent of the budget.

5.6 Infrastructure Building

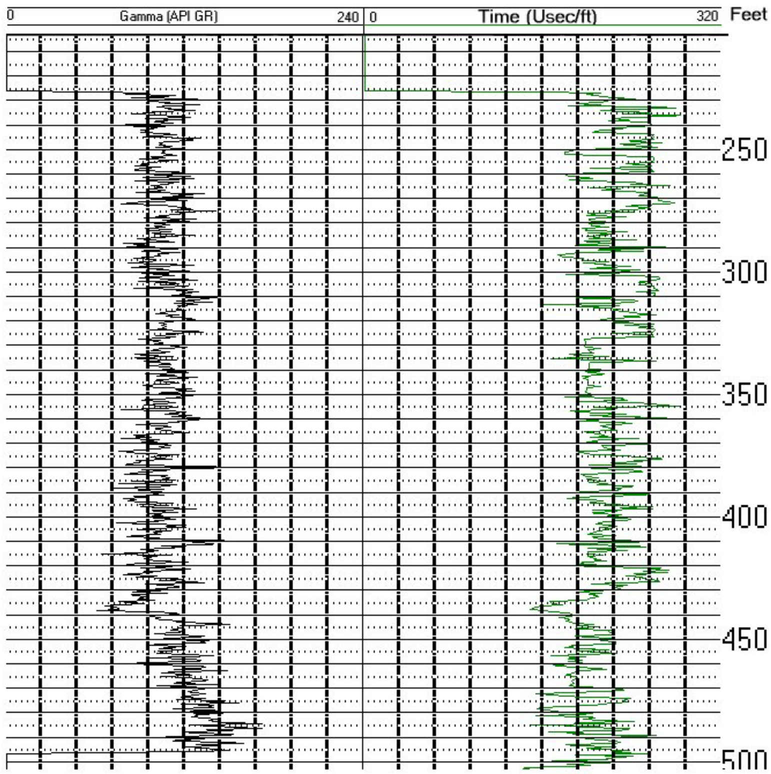

Figure 5-2. Example of an electric log in the lower portion of the Presho #2 hole (southeast of Presho, SD). The left curve is the natural gamma ray response, which is an indicator of lithology, and the right curve is the interval travel time, which is an indicator of porosity. The sonic curve was generated using the new sonic logging tool acquired during the course of this project. Electric logging was performed by the DENR-SDGS.

The project provided assistance toward the purchase and addition of capabilities for two major items. These included an allocation of $51,000 toward an additional capability for the triaxial testing instrument in the Department of Mining Engineering and Management at SDSM&T. The triaxial testing equipment is able to measure the rock mechanics properties of samples under stress and will now be able to also measure the sonic velocities under stress as well. This equipment was used in the current project and will continue to be an invaluable tool for further studies. The triaxial testing system is described in detail in Appendix B, Description of New Triaxial Testing Machine.

The second major investment amounting to $20,300 was to purchase a sonic logging tool to determine downhole of acoustic velocities of the *in situ* shale and to allow correlation of the properties between laboratory measurements and the shale in the subsurface (Fig. 5-2). This instrument compliments the current electric logging suite of the DENR-SDGS where it will reside. This instrument was useful in the current study and will continue to be of use in a wide range of environments in the subsurface where porosities need to be determined, e.g. ground water studies. Both equipment purchases were used in the current project and will continue to be invaluable tools for further studies.

6. Report Contributors

The following individuals contributed to the report, including: W. Roggenthen[1], L. Roberts[2], A. Chowdu[2], A. Freye[1], E. Melville[1], D. Malinzak[1], J. Nopola[3], J. F. Sawyer[1], L. Stetler[1], and P. Tukkaraja[2]. Their written contributions are appreciated greatly as was the assistance during the field operations, which involved preparation of core material and geologic logs.

[1]Dept. of Geology and Geological Engineering
South Dakota School of Mines and Technology
501 E. St. Joseph Street, Rapid City, SD 57701

[2]Dept. of Mining Engineering and Management
South Dakota School of Mines and Technology,

[3]RESPEC, Inc.
3824 Jet Drive
Rapid City, SD 57703

APPENDICES

APPENDIX A Geomechanical Laboratory Analyses

A1. Geomechanical Sample Acquisition

The necessity to obtain fresh shale samples for analysis is rooted in the sensitivity of the Pierre Shale to both mechanical and chemical weathering. The Pierre Shale that exists near the surface across much of western South Dakota has been altered to such a degree that the mechanical, hydrological, and chemical properties (as well as the visual appearance, in many instances) cannot be considered representative of the unaltered shale at depth. Further complicating analysis of unaltered Pierre Shale is the propensity for alteration as soon as the rocks (which have never been subjected to an oxygenating environment since their deposition in a deep marine setting) are exposed to air. Therefore, even when intact samples are acquired from depth (such as previous core that exists at the South Dakota Geological Survey Core Archive), the rapid weathering processes of these materials renders them unsuitable for meaningful mechanical, hydrological, and chemical analysis.

The overarching goal when trying to successfully sample shale is to maintain the in situ conditions as much as possible, including mechanical, hydrological, and chemical conditions.

- Mechanical: samples that are suddenly removed from a certain stress state (such as through boring acquisition) may become damaged, e.g. disking.
- Hydrological: shales are composed of clay minerals which are often prone to bulk volume change as the water content changes. In weak rocks such as the Pierre, changes in moisture content can affect the physical properties of the sample.
- Chemical: exposure to oxygen can cause a chemical reaction in rocks that have originated in a reducing environment. This can affect the chemical composition of the sample and the appearance. Additionally, pore water geochemistry may be lost upon drying.

The main objective when preserving shale samples obtained from depth is to maintain the original moisture content and limit exposure to air. Three different preservation methods were used to fulfill these tasks, as follows:

- Saran Wrap: core was wrapped in Saran Wrap before being placed in PVC tubes. This process was relatively straightforward, but there was some difficulty in maintaining a complete seal. One-half of the Tree Dam core was sealed with this method, primarily to be used for hydrocarbon analysis.
- Mineral Oil: core was placed in a sealed PVC tube and immersed in inert mineral oil. This is perhaps the best means of long-term preservation but is very messy and sampling can be difficult. Half of the Tree Dam core was sealed with this method, primarily to be used for mechanical testing.
- Argon Gas: core was flushed with argon gas before being vacuum sealed in polyline tubing. This method may have been the most overall successful, considering ease of effort and degree of preservation.

A2. Advanced Geomechanical Laboratory Testing

Multiple efforts were undertaken related to laboratory testing of the newly acquired Pierre samples including mechanical tests, microscopy, mineralogy, and micropaleontology.

Mechanical tests require the preparation of specimens that are in a perfectly cylindrical shape, preferably with the sample height twice that of the sample diameter, so that uniform stress conditions are achieved during the testing process. While preparation of samples may be a seemingly minor process, it was anything but trivial working with the weak Pierre Shale. Innovative methods had to be developed so that competent samples could be created. In many instances, despite significant and admirable efforts, the core was somewhat damaged by the drilling, preservation, and transportation process. Namely, breaks across the diameter of the core were common and often coincided with bedding planes of the samples. These breaks were very often closer than what would be desired for mechanical tests specimen (a 2:1 ratio) and were many times far too close to even consider making a test specimen (spacing of about 2 inches). Additionally, many potential samples were damaged during the specimen preparation process. The lessons from the specimen preparation process eventually resulted in techniques that provided the best chance of success for sample preparation. Briefly, some of the items are:

- Custom-made specimen clamps that provide confining pressure during sample cutting
- Vacuum system for jacket placement around the sample
- Subcoring of Pierre samples is not practical, despite the use of a “damped” drill which has proved useful on more indurated shale
- Successful sample preparation was much easier to achieve in the more massive units (namely the Verendrye Member) than the fissile units (such as the Virgin Creek and De Grey Members).

Additional triaxial tests are proposed and the results of the completed tests are displayed in Figure A-1. Although more detailed analysis of these results is ongoing, the following preliminary observations can be made:

- In general, the triaxial strength of the preserved samples (this study) is reasonably close to the strength of previous studies where weathered or inadequately stored samples were used, although there is less scatter in the data from this study. This observation is somewhat surprising and further investigation into sample acquisition methods for the previous studies is ongoing.
- A certain amount of scatter in the cumulative data set is apparent. Initial theories were that the individual members of the Pierre may possess different strength criteria. However, the difficulty with specimen preparation for the fissile units prevented acquisition of a statistically viable sample size for individual fits (most successfully prepared samples were from the Verendrye Member). Further investigation into the influence of individual members for both this study and previous studies is ongoing.
- The core from the different hole (and different preservation techniques) does not appear to have an obvious influence on the strength of the samples.

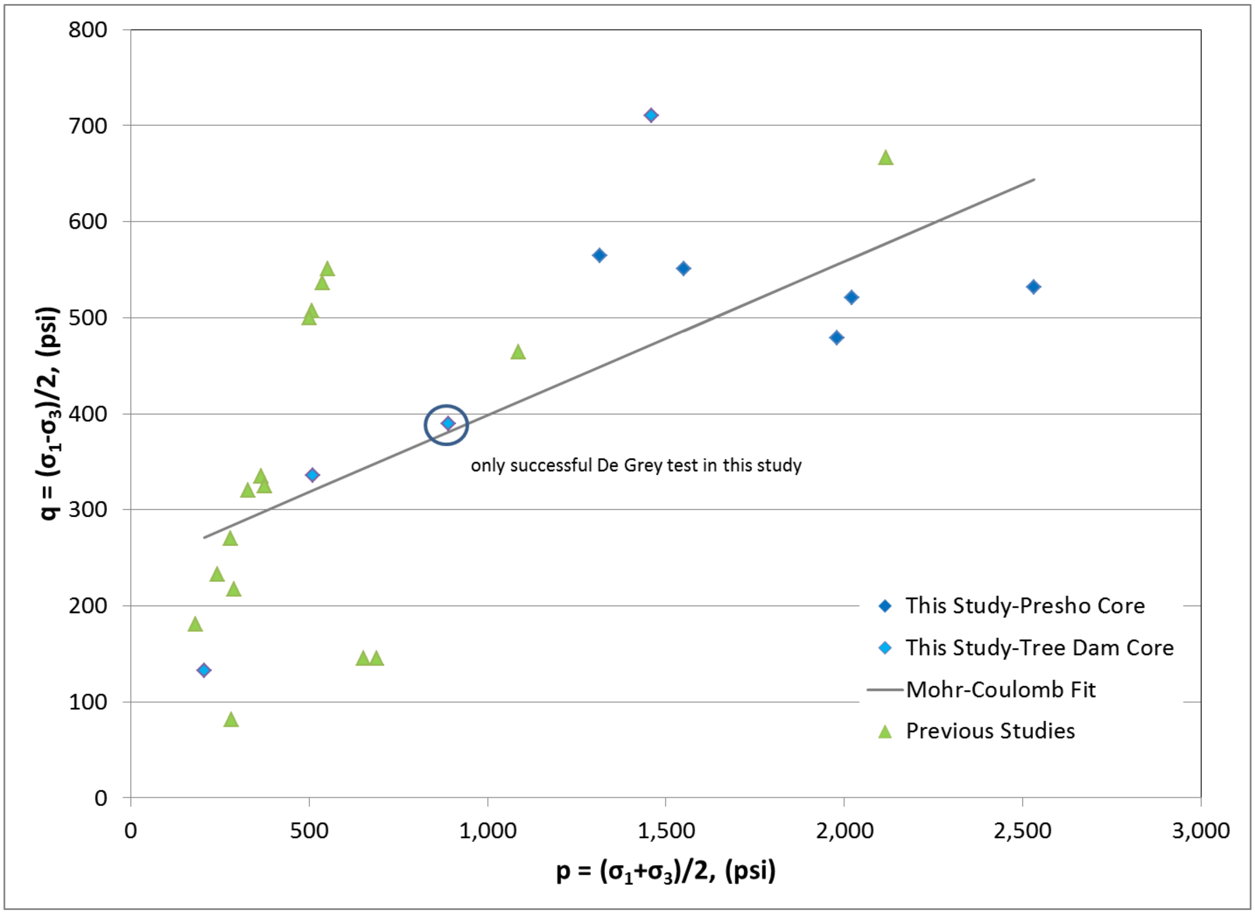

Figure A-1. Modified Mohr-Coulomb "p-q" Plot and Data Fit for Peak Strength. C=241 psi and phi = 9.2 degrees.

The information obtained from the strength tests is important in understanding the influence on the long-term deformation behavior of the shale. The current work has been focused on identifying the "peak" strength of the shale, which is to say the maximum stress difference that the samples reach before completely failing and weakening (termed residual strength). Understanding the limit of linear (or perhaps non-linear) elasticity is also important in understanding time-dependent deformation. The elastic region is where changes in stress do not produce permanent damage; the sample will rebound to its previous shape once unloaded. Within the elastic region, long-term deformation is not expected, as any long-term deformation in the shale is presumed to be a plastic, non-recoverable process. The triaxial tests can be used to identify both peak strength and the yield stress (after which permanent plastic deformation occurs). An example of a single triaxial test (equivalent to one of the "dots" in Figure A-1) is shown in Figure A-2. The peak strength is easy to distinguish; however the yield stress location is very subtle. Mathematical techniques will be used to aid in selection of the yield point where plastic deformation occurs. A plot similar to Figure A-1 will then be produced identifying the criteria for yield. One of the possibilities being considered is that the yield stress is essentially immediate (i.e., any stress difference creates an irreversible change in the specimen). This approach is closer to soil mechanics than traditional rock mechanics and accentuates the overlap of disciplines required when evaluating these weak rocks, sometimes termed intermediate geomaterials.

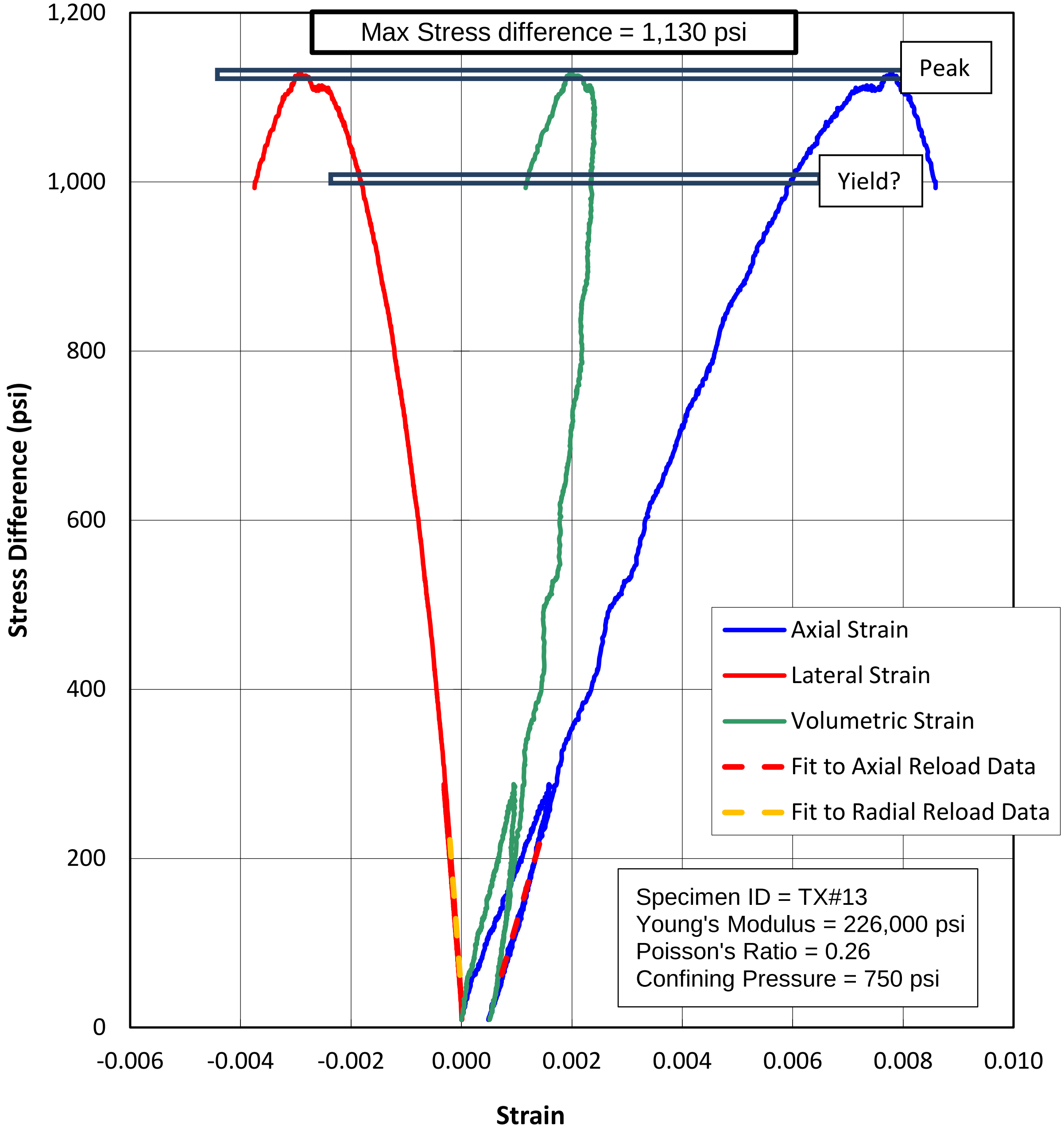

Figure A-2. Triaxial Stress-Strain Plot for Specimen ID TX#13.

Triaxial constant stress difference creep tests were performed on the samples to evaluate their time-dependent deformation properties. While shale creep tests performed by others have been reported in the past, previous tests are considered somewhat lacking because of the testing apparatus (often uniaxial tests or constant load tests) or the test duration (often performed only hours to a few days). The testing procedure for this study was unique both because of the state-of-the-art equipment used (triaxial constant stress difference machines) and the duration of the tests (often several weeks). A total of seven long-duration creep tests have been performed with additional tests still planned. As previously mentioned, preservation efforts were made with the intent to limit changes in moisture content to the sample and introduction to air. The preservation efforts were maintained throughout the sample preparation process.

The effect of pore water on the testing can be important, e.g. poromechanics. As saturated specimens are rapidly loaded, porewater can support some of the load, reducing the effective stress (total stress minus porewater pressure) which makes the samples more likely to fail. If the excess porewater can drain from the system (a drained test) the specimen matrix can again support the load (as opposed to the pore water) which increases the effective stress and makes the sample more stable. All of the creep tests were performed under drained conditions to allow excess pore pressure to dissipate between stages. When a sample is initially loaded, the porewater pressure is at its highest and the sample is most likely to fail. As time passes, water can drain from the system and the entire load is again supported by the specimen matrix. The shale has a low permeability and therefore it takes considerable time for the water to drain from the system. The drained conditions and a series of staged stress difference applications (generally about 100 psi) over several days was used to limit excess pore pressure buildup which could cause the specimen to fail.

The results of the creep tests are still preliminary at this point and need to be processed further, but some of the initial findings are presented herein. Total axial strain versus time is presented in Figure A-3 and Figure A-4 for two different specimens. The specimen shown in Figure A.3 was tested with 1,000 psi of confining pressure while Figure A-4 was tested under 2,000 psi of confining pressure. The samples were placed under isotropic stress conditions (confining pressure equal to axial pressure) for several days prior to the initial stress difference application to allow consolidation of the specimens. Each “step” in the axial strain represents an increase of approximately 100 psi in the stress difference. Figure A-3 is a sample from the upper De Grey Member of the Pierre (generally a thinly bedded fissile shale) and Figure A-4 represents a sample from the Verendrye (typically a more massive mudstone). While more work needs to be performed to evaluate other potentially influential contributing factors, the difference in creep response between the two members is notable. Figure A-3 displays a significant axial strain, eventually exceeding 20%. Despite the massive strain the specimen never reached a point where it failed catastrophically, instead continuing to gradually deform. This test was eventually stopped and the final sample removed was largely a disintegrated rock mass held together by the specimen jacket, as shown in Figure A-4. By contrast, Figure A-5 displays an axial response of only about 1% after a similar duration and stress path. Much of the difference between the overall axial strain magnitude in the specimens displayed in Figures A-3 and A-5 appears to be related to the immediate response after additional load is applied. The axial strain rate, also displayed in Figures A-3 and A-5 is relatively similar between the samples (typically ranging between $1\text{x}10^{-9}$ and $1\text{x}10^{-11}$ /second) with the strain rate generally increasing with increasing stress differences.

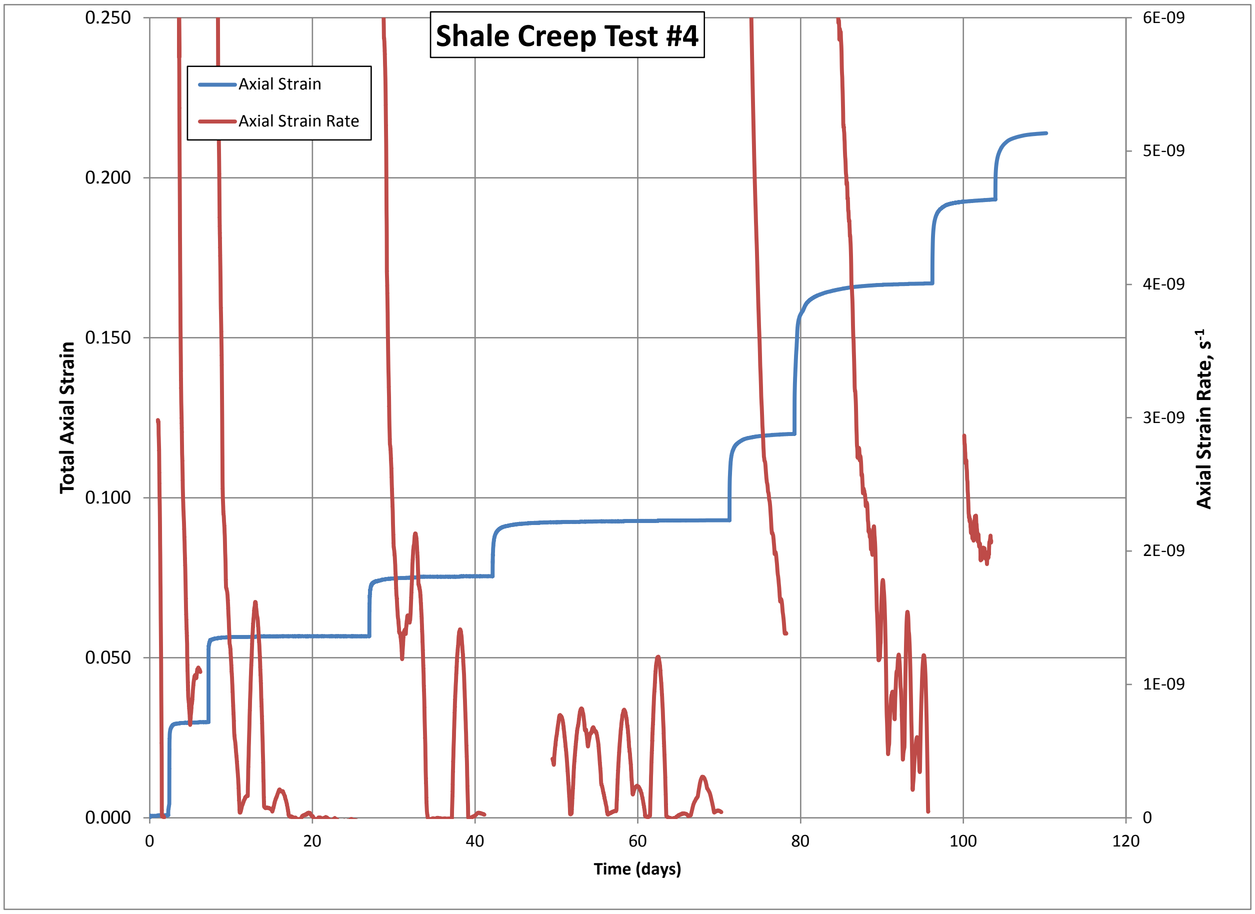

Figure A-3. Triaxial Constant Stress Difference Test of Axial Strain and Axial Strain Rate versus Time for Specimen CT#4.

Figure A-4. Post-test Photo of Specimen CT#4 Illustrating a Largely Disintegrated Rock Mass Contained Within the Specimen Jacket.

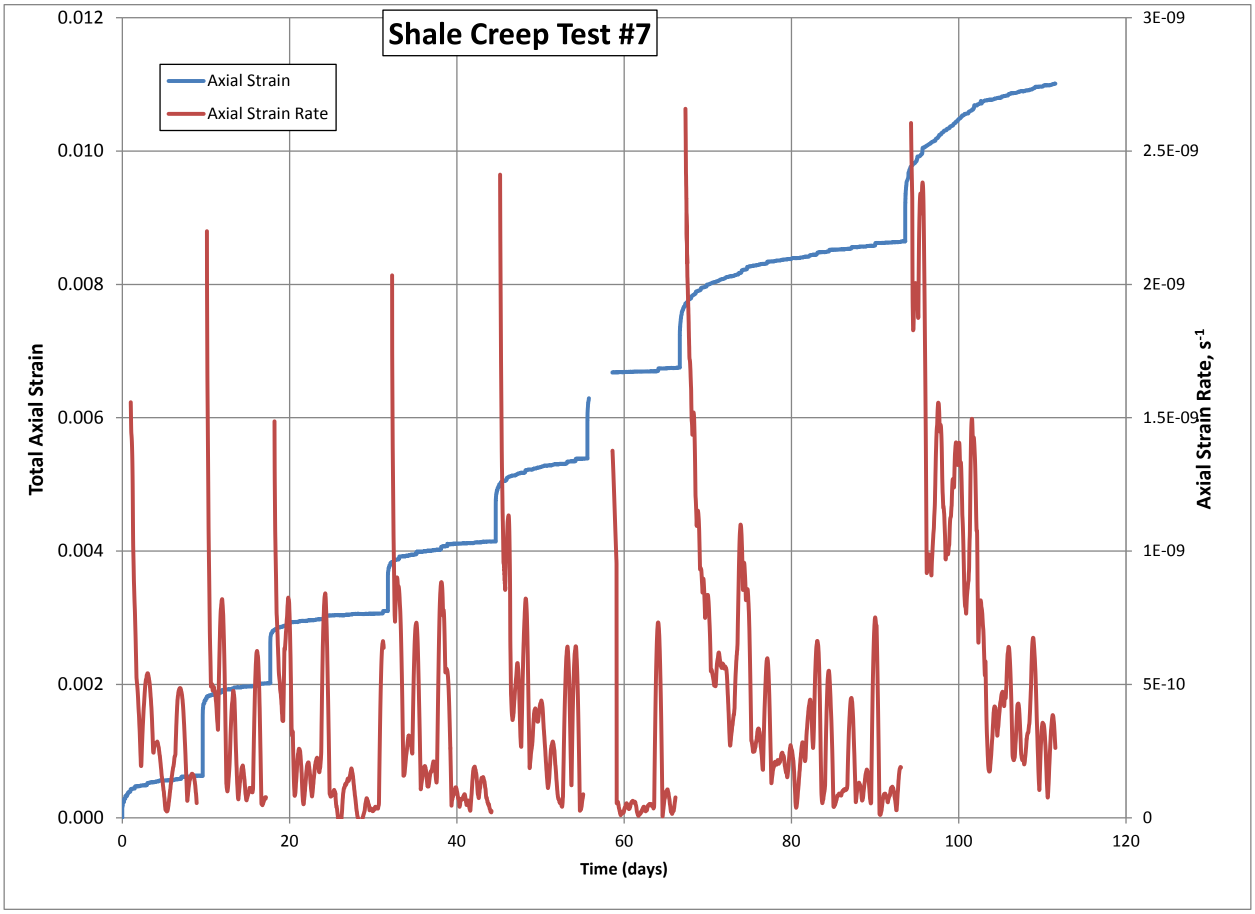

Figure A-5. Triaxial Constant Stress Difference Test of Axial Strain and Axial Strain Rate versus Time for Specimen CT#7.

Whereas the samples presented in Figures A-3 and A-5 were maintained several weeks under increasing stress differences, other samples experienced failure at much lower stress differences. Total axial strain versus time is presented in Figure A-6 and Figure A-7 for two different specimens that experienced very different failure mechanisms. The specimen shown in Figure A-7 was tested with 1,000 psi of confining pressure whereas Figure A-6 was tested under 2,000 psi of confining pressure. Both failed under a stress difference of 200 psi. The sample in Figure A-6 experienced an accelerating failure over several days, while the sample in Figure A-7 failed very suddenly. The influence of pore pressure on these failures is certainly being considered, but at face value the importance of its influence is somewhat questionable, at least in CT#2, as the pore pressure would be greatest immediately after load application and decrease thereafter.

The response of these tests, as well as that of the other tests, will continue to be evaluated as the research progresses. Efforts are currently underway to attempt to calculate the volumetric and radial strain of the samples based on the volume of fluid in the confining vessel. This method is necessary because of the inability to subcore the samples. The larger sample size prevents the ability to use radial strain gauges because they cannot fit in the vessel.

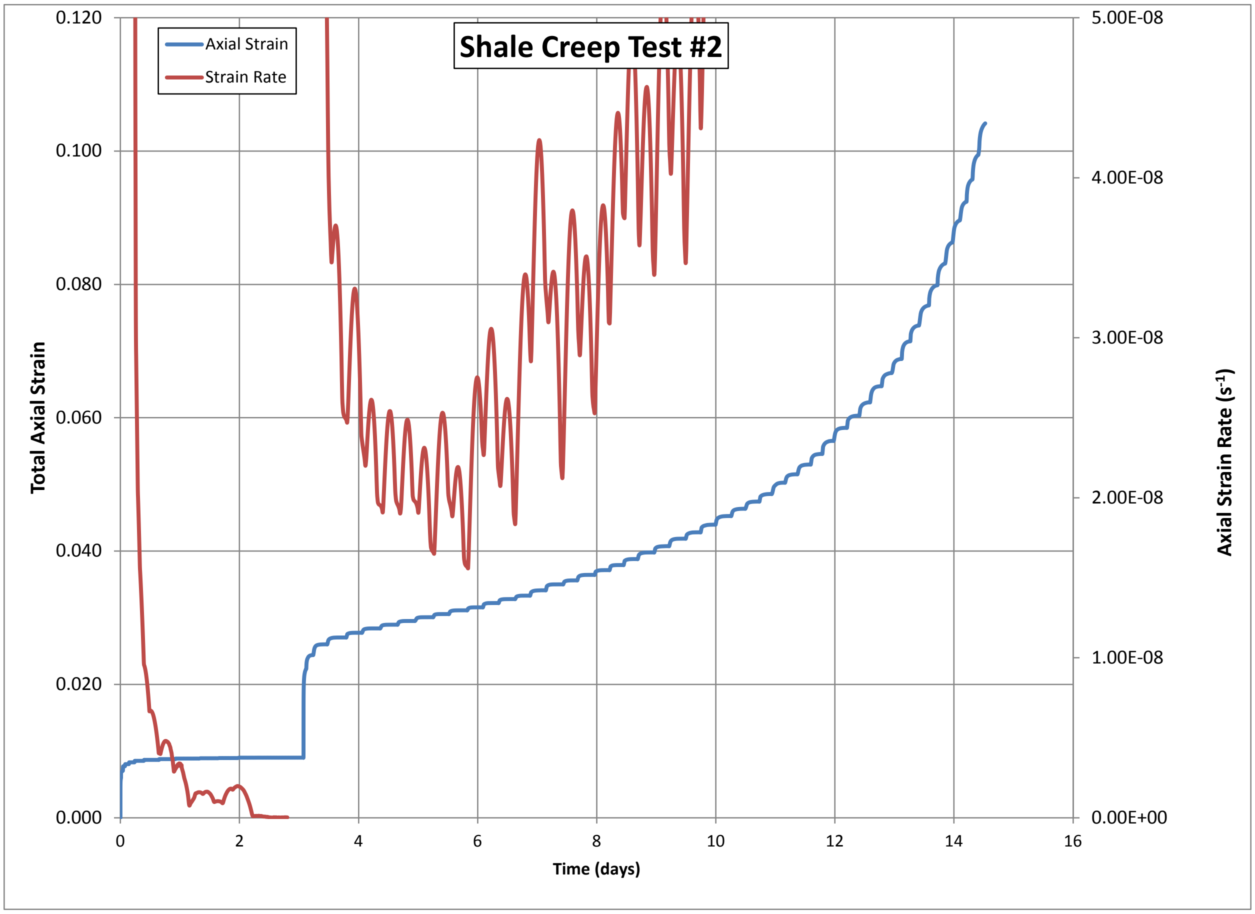

Figure A-6. Triaxial Constant Stress Difference Test of Axial Strain and Axial Strain Rate versus Time for Specimen CT#2.

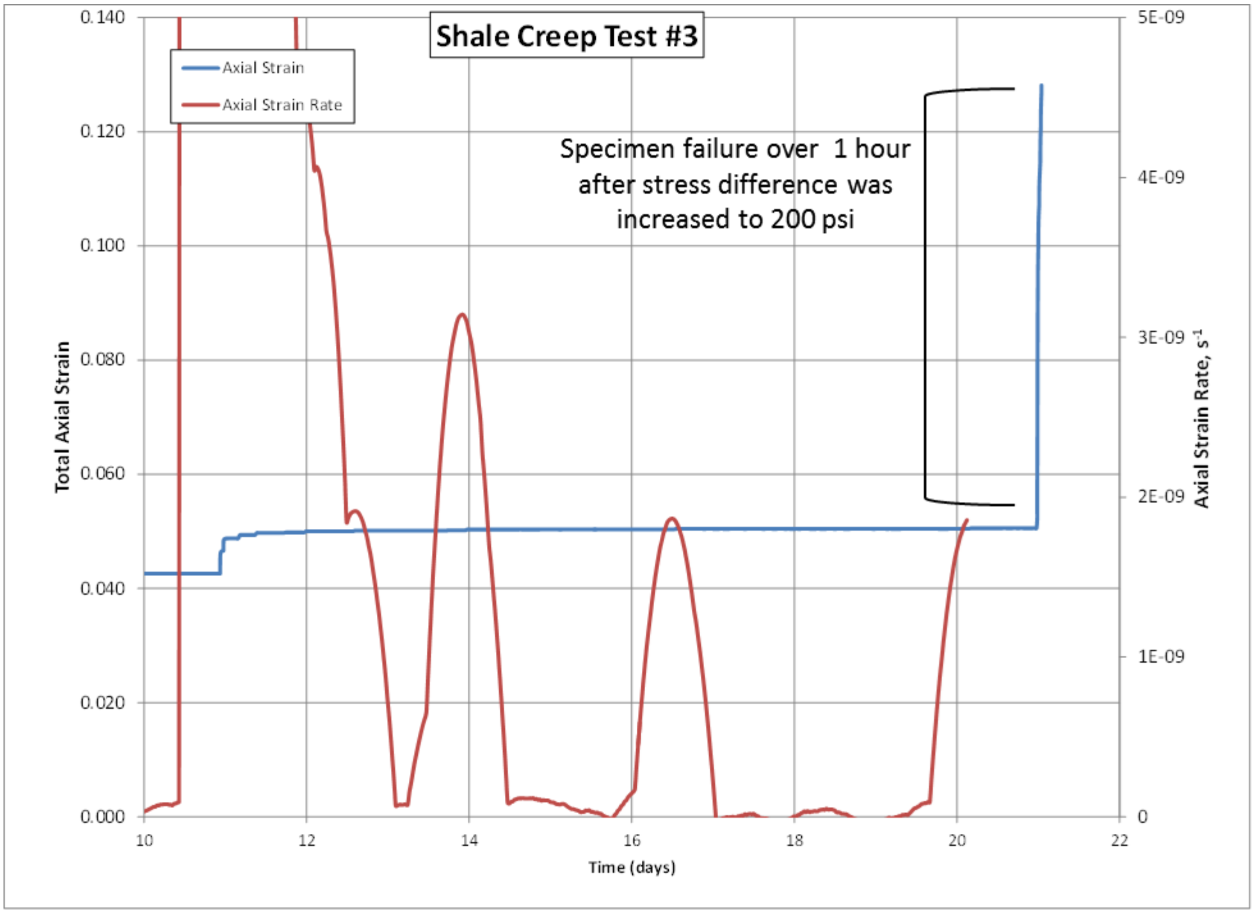

Figure A-7. Triaxial Constant Stress Difference Test of Axial Strain and Axial Strain Rate versus Time for Specimen CT#3.

A3. Transferability of Constitutive Models for Geomechanics

Constitutive modeling efforts have thus far focused on the capabilities of existing, established constitutive models to predict the behavior in the test specimens. FLAC3D has been used to evaluate the poromechanical response of replicated test specimens using the physical properties (and often a range of physical properties) determined for the Pierre Shale from both this study and previous studies. These preliminary scoping studies use a quarter-specimen replication of the lab tests with the diameter and height for each model. The specimen is assumed to be initially saturated and the tests are simulated as drained. One example of the many numerical simulations of Test CT#2 is displayed in Figure A-8. Included in Figure A-8 are both an isometric view of the test model and a graph of axial strain versus time. The x-axis is time in seconds and therefore the entire simulated duration is about 23 days. Figure A-8 includes the initial specimen consolidation which is not shown in the creep test results in Figure A-6.

The numerical modeling effort is ongoing but the preliminary results indicate that the long-term creep test response cannot be simulated using poromechanics only. Figure A-9 displays a comparison between the measured and calculated axial strain for CT#2. Despite decreasing the modeled elastic properties by an order of magnitude compared to the measured laboratory values (in an attempt to increase the initial elastic response), the general axial response is not well matched. Additionally, the numerical models do not predict any plastic failure, which appears to be occurring gradually during the period of accelerating creep rate. The modeling effort will continue to investigate more advanced models for time-dependent damage accumulation and, if necessary, develop new methods of simulating the observed response.

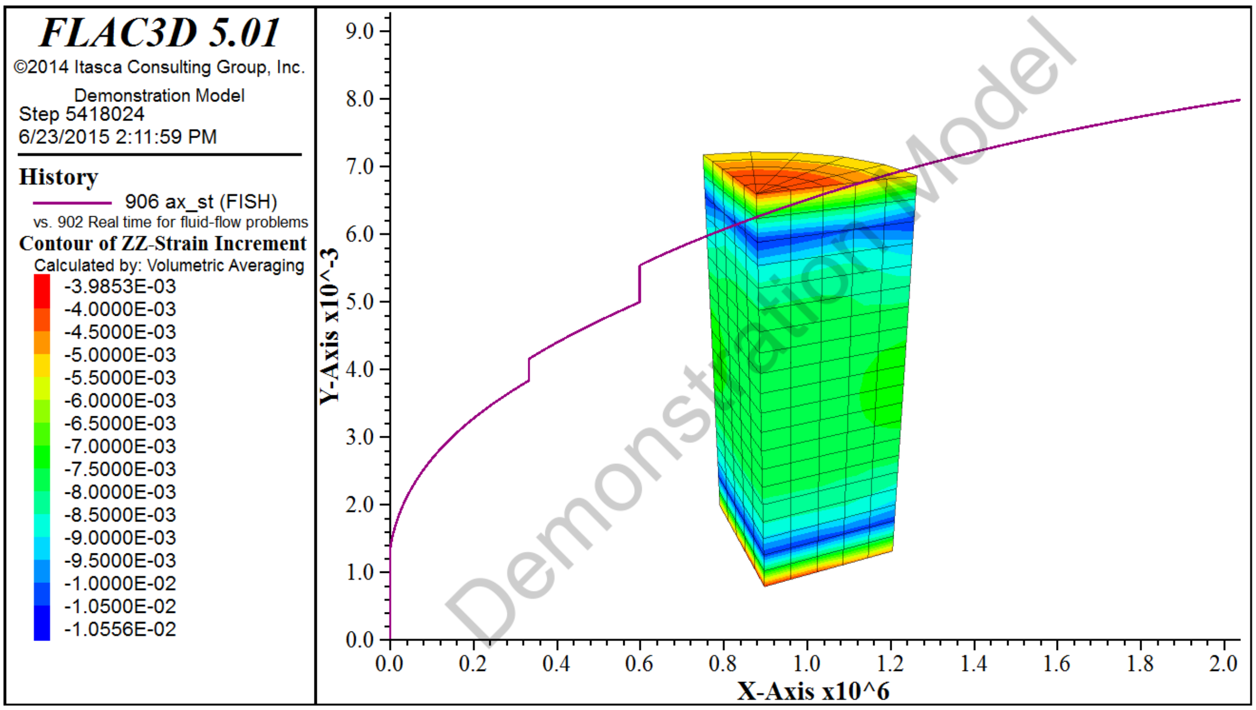

Figure A-8. Example of Numerical Modeling Results for Axial Strain of Specimen CT#2.

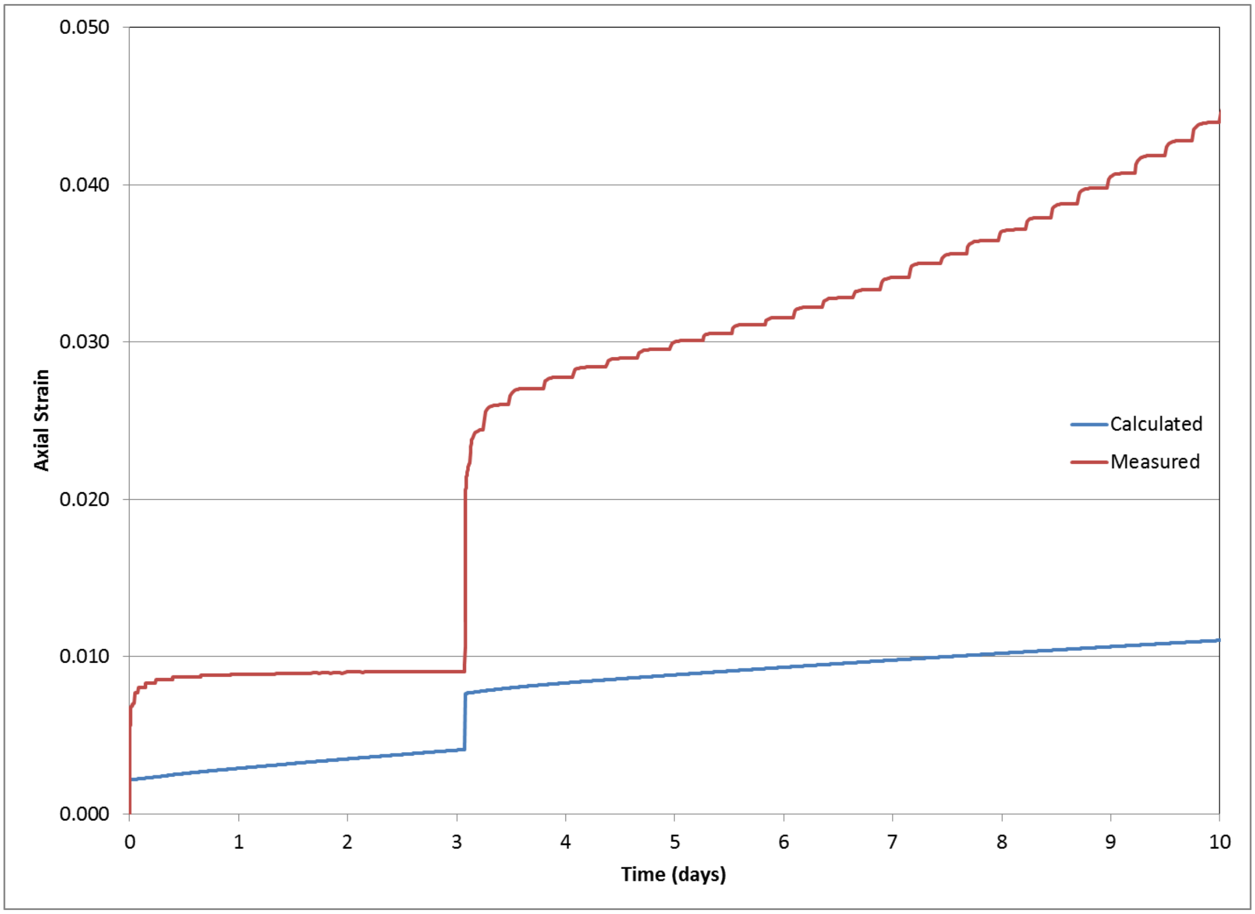

Figure A-9. Comparison of Measured and Calculated Axial Strain versus Time for Specimen CT#2.

APPENDIX B Description of New Triaxial Testing Machine

B1. General Principles

The GCTS Rapid Triaxial Rock - 1000 Testing System (Fig. B1-1) is a state-of-the-art testing apparatus designed to determine the mechanical and hydrological properties of soft to hard rocks under simulated underground conditions. The system has been highly optimized for single-operator testing, requiring significantly less downtime during sample preparation. The complete system consists of essentially five different components, as shown in the picture below.

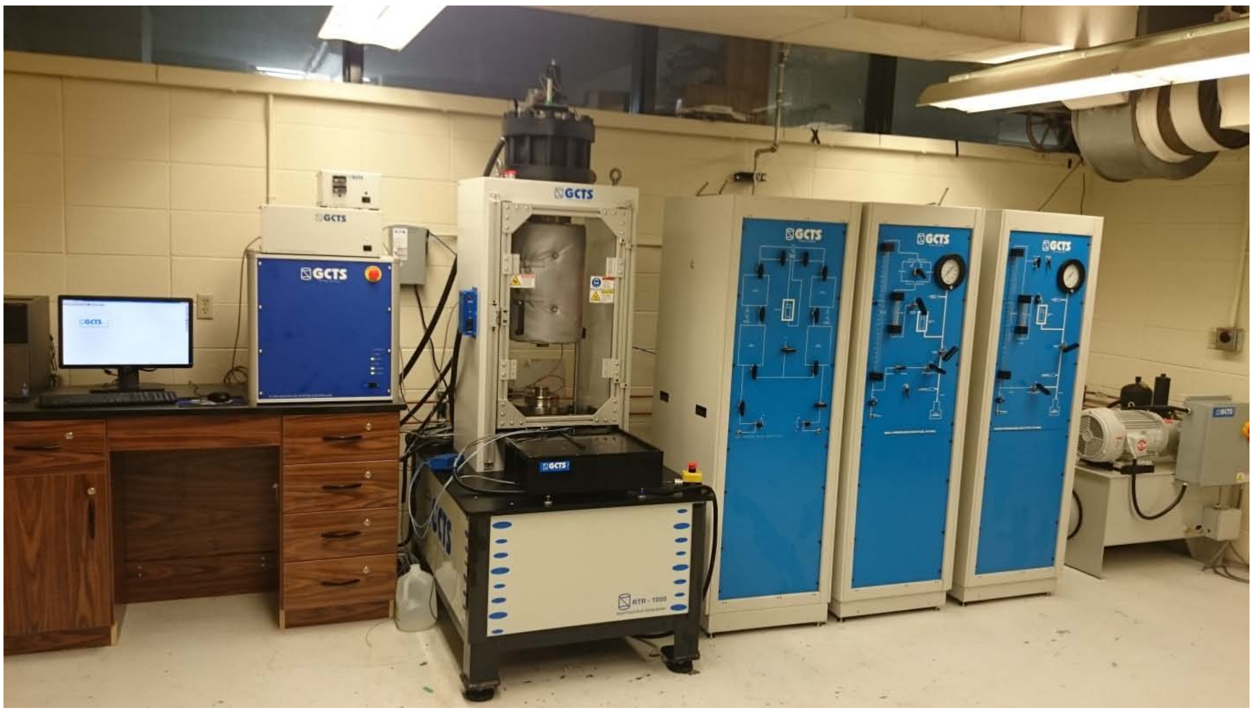

Figure B1-1. GCTS RTR-1000 Testing System

B2. Individual Components

The specifications for each of the individual system components are described below:

<u>Load Frame</u>

The load frame is rated for a 250,000 lbf static and an 180,000 lbf dynamic maximum axial load with a 2-inch piston stroke. It also features a high system stiffness of 10,000 lbf/mil. Any friction during piston movement is minimal and is automatically compensated for by the system. The cell wall is rated for a maximum 20,000 psi confinement pressure and 300° F temperatures. The cell can accommodate samples up to 3” in diameter and twice in length. Cell assembly is quick & easy, affected through a hydraulic piston setup with an AutoLock feature.

Currently, the system is equipped with a 250,000 lbf internal compression load cell with a spherical seating setup. It is rated to operate under the same testing conditions as the cell wall. Only samples of NX (2”) and HQ (2.4”) can be tested at this moment. Axial and circumferential deformation measurements are affected through supplied LVDTs with a range of +/- 98 millinches. These are mounted to the specimen using two holder rings, which can accommodate, at most, an HQ-sized specimen. An example of the specimen mounting procedure is shown in Figure B2-1. For larger specimens, the frame deformation LVDT can be used for axial measurements, which has 0.001” resolution. Lastly, to accommodate short specimens, spacers can be added to the piston to further increase its reach.

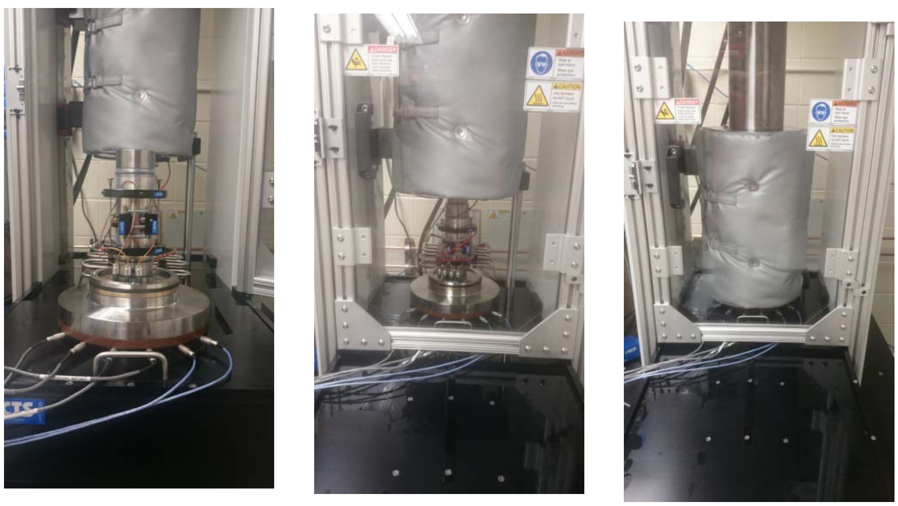

Figure B2-1. Example Specimen Mounting.

a. <u>Digital Control & Acquisition Unit</u>

This component actually consists of two separate units, namely the CATS Advanced software and the SCON-2000 Digital Servo-Controller. The former provides a user-friendly graphical interface to operate the machine, while the latter actually controls the entire system. During a typical test, the procedure will be programmed in using the CATS software. This is then transferred to the SCON unit once the test begins and will continue to run, irrespective of whether the CATS software is running or not. All incoming transducer signals are received at the SCON and conditioned, before being transferred to CATS in real-time. The SCON comes preconfigured with 19 transducers/inputs for various parameter measurements and five outputs for controlling the system. These can be further expanded up to 28 inputs and eight outputs, respectively.

The CATS software is fairly advanced and provides for a high amount of customization (Fig. B2-2). Test setup is quick and the software provides for four types of testing phases: Consolidation, Static Loading, Dynamic Loading and Universal. The first three are mostly pre-configured, requiring some user input, and the last can be used for more complex testing procedures. By default, about 20 pre-programmed test parameters are provided to monitor any test. Custom functions to calculate new parameters can be further added, to supplement the existing ones. All calculations are done in real-time and displayed almost simultaneously on the operator’s screen. Also, manual control of the system is available, either via a directly measured parameter or a calculated parameter. Besides system control, the software also incorporates some useful tools for cataloging the various tests and for quick analysis of the test results.

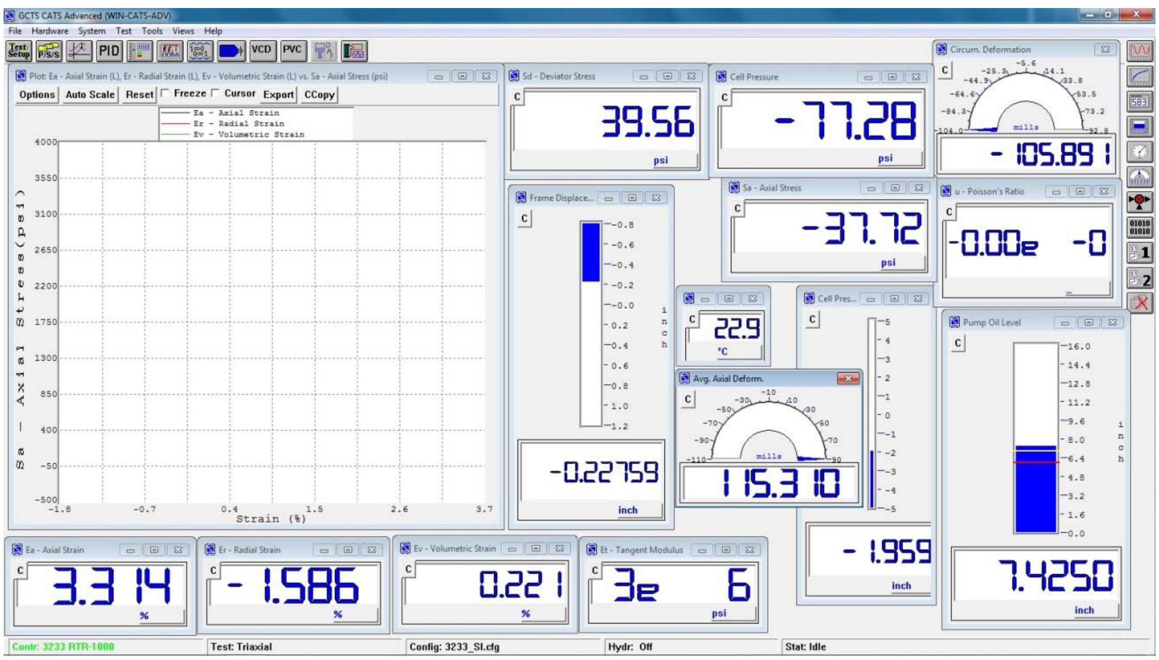

Figure B2-2. CATS screen used for monitoring a typical Triaxial Test

b. <u>Hydraulic Pump and Cell & Pore Pressure Cabinets</u>

The Hydraulic pump is the main source of hydraulic pressure for the entire system. It operates at two pressures – Low (1000 psi) and High (3000 psi) and is controlled via the CATS software. It runs in a closed loop and has a 150-liter capacity tank.

The pressure supplied by the pump goes to the Cell & Pore Pressure (CP & PP) Cabinets, where it can be further stepped-up, using Intensifiers, to 20,000 psi each. The CP unit has a 560 cc operating volume, while the PP unit has 280 cc volume. Both can be refilled during testing also, if required, from the provided five gallon backup reservoirs. Manual piston control can be affected via the CATS software, using a linear transducer as the controlling parameter. Vacuum and Low-Pressure (100 psi) systems are provided for rapid filling/emptying of the triaxial cell and the specimen (saturation/draining in this case).

c. HPPD Cabinet

The Fast Pulse-Decay Permeability Apparatus is designed to measure the permeability of micro-porous material such as gas-shale and other reservoir rocks, in order to determine the capacity and flow characteristics of the rock matrix. It has a resolution of 1 µD (microDarcy) and comes with two sets of two 500cc and 2000cc reservoirs. A needle-valve is used to produce a maximum pressure difference of 300 psi across the top and bottom of the specimen. All the components are accommodated in the insulated metal cabinet to reduce errors due to expansion and contraction of the fluid.

d. Ultrasonic and Temperature Controls

The system capabilities have been further expanded to include Ultrasonic and Temperature controls. The ULT-100 system can be used to determine the elastic properties of the specimen under the simulated conditions by utilizing ultrasonic wave velocity measurements. The system is similar to the SCON-2000 unit, operating independently of the CATS software. The sampling rate can be selected from 20 MHz to as low as 156 Hz, allowing the user to capture a wide range of ultrasonic signals. Various pre-programmed filters are also provided to clean up the signal and custom ones can be further added in. Currently, the system can only accept NX size specimens for such a test. Another feature of the system is that tests can be conducted at elevated temperatures to more closely simulate underground conditions. All equipment used within the triaxial cell is rated for safe operation until 300° F. Temperature measurement is affected using two thermocouples, one located internally and one on the cell wall. This helps to minimize overshoot and control temperature gradients within the cell chamber.

e. Safety Controls

Each individual system component has built-in safety controls to protect both the user and system from any adverse mishaps. Emergency STOP switches are provided at various places to affect an immediate stop on all the component operations. Basically, all components will start reverting to pre-test conditions. All pressurizing devices are provided with safety-release valves that, once activated, are equivalent to a STOP switch. In case of a loss of system power, the hydraulic pump pressure is immediately lost. The CP & PP cabinets will continue to hold pressure, though this will also start bleeding off slowly.

B.3. Testing Capabilities

A number of tests can be performed using the above system on rock specimens.

1. Triaxial Test with Static & Dynamic Loading
    a. Unconsolidated - Undrained

b. Unconsolidated - Drained

c. Consolidated - Drained

2. Uniaxial Compressive Strength Test
3. Permeability Test
4. Ultrasonic Wave Velocity Measurement

Below is an example of the results obtained during testing of the Shale sample TX# 13 (Fig. B3-1). The test was conducted at 750 psi confinement pressure and the specimen failed at an axial stress equal to 1878 psi.

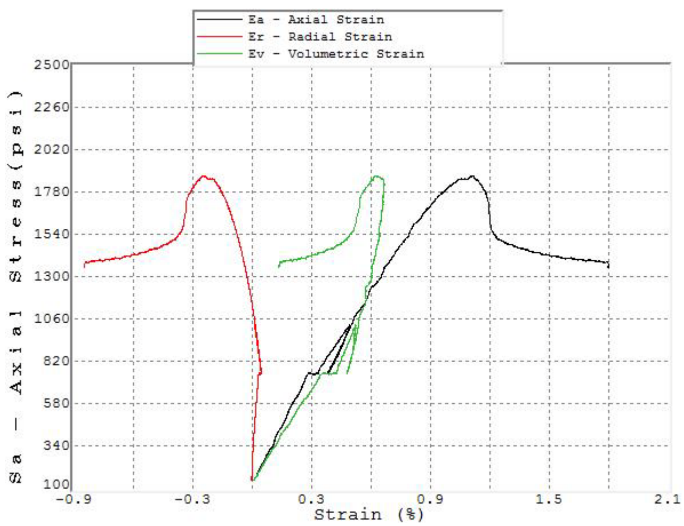

Strain vs. Axial Stress graph as obtained via GCTS CATS software

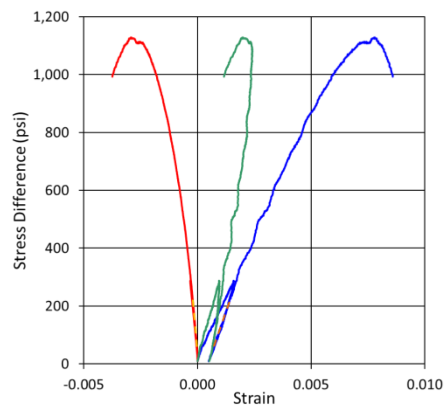

Strain vs. Deviator Stress graph as obtained via Excel

Figure B3-1. Plots of strain against axial stress and strain against deviator stress.

APPENDIX C Computer Tomography and Scanning Electron Microscopy

C1. CT Scanning of Shale Core Materials from South Dakota

Computed Tomography, a method for producing high-resolution imagery from exposing samples (bone and tissue) to high-energy X-rays, was originally developed for uses in the medical industry. CT, or CAT, scans utilize a radioactive source and a detector. A sample is placed between the X-ray source, which often is cesium, and the detector. The sample is bombarded with X-rays that are collected or counted in the detector, which measures the attenuation of X-rays passing through the sample. This attenuation is a function of original X-ray energy, sample density, and average atomic number of material making up the sample. As the method became a standard medical evaluation tool, other uses for CT scanning were developed, including the method of seeing inside of rock materials, specifically, imaging the grain density and pore spaces. For rock samples, imaging grain structure required higher X-ray energy (>100 keV) and long exposure times (hours instead of seconds). This led to the development of CT scanners, which are capable of imaging to the micro scale (10^{-6} m).

As for medical scanning where the scanner rotates around the sample, an arm for example, to derive a 3D image of the arm, micro CT scanning rotates the sample between the source and detector. Each separate image during the scan represents a 2-dimentional image (Fig. C1-1), and all of the individual image slices are put together at the end of the procedure to produce a full 3-dimensional image (Fig. C1-2). The size and resolution of the 3D elements are dependent on the detector used and the distance the sample is away from the detector.

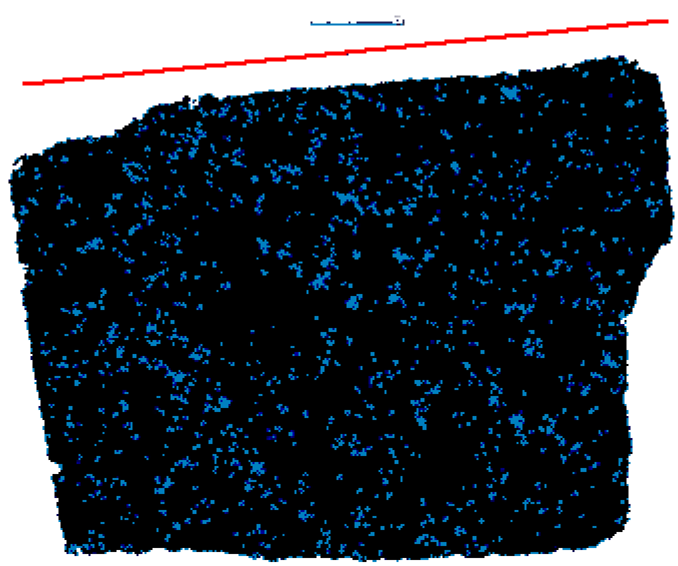

Figure C1-1. Two-dimensional X-ray image of sandstone using the XRadia (Zeiss) Micro400 CT scanner at SDSMT. Dark areas are solid quartz grains and the blue areas are the hollow pore spaces between the grains. The red line is approximately 4 mm in length.

C1.1 Scanning Process:

Developing a CT image of a rock sample involves four components; sample preparation, scanning, image reconstruction, and density segmentation. Sample preparation for CT scanning requires samples from either outcrop or core to be cut with a rock saw or broken into small rectangles roughly 4-5 mm in thickness and attached to a steal rod with super glue adhesive (Fig. C1-3). The sample is located between the source and detector (Fig. C1-4) and various filters are placed in front of the source based on the sample protocol, X-ray energy, and image resolution desired.

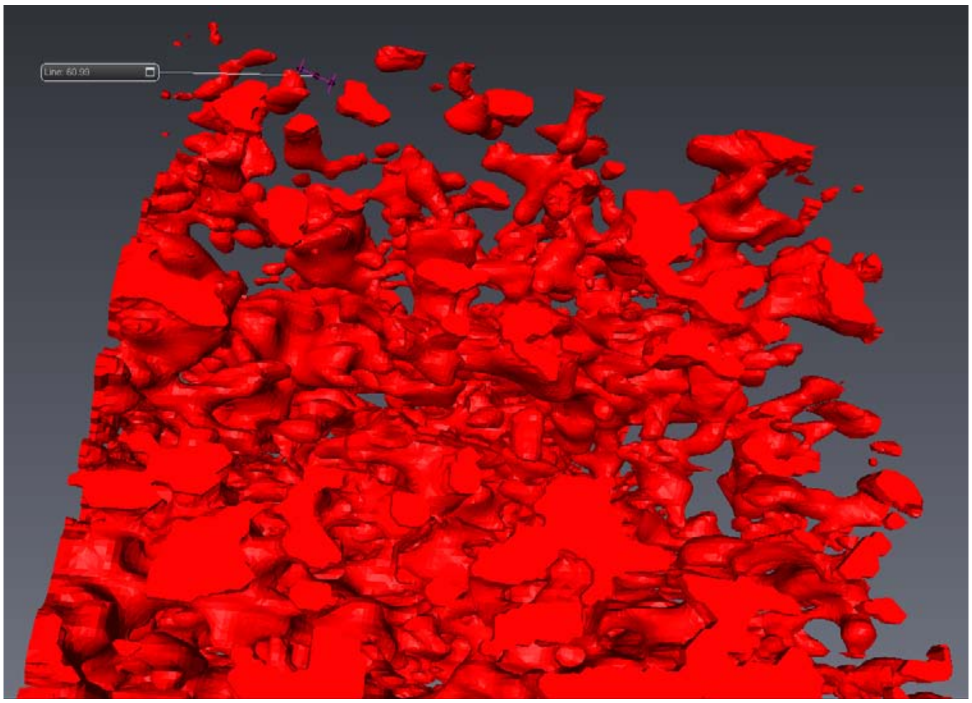

Figure C1-2. Three-dimensional X-ray image of sandstone using the XRadia (Zeiss) Micro400 CT scanner at SDSMT. Red areas are pore spaces between the grains. The scale line is approximately 61 μm (micro meters) in length. The pore space appears to be near 100% toward the bottom of the image and is due to the 3D view, i.e., the view is into a volume. Spaces that grains occupy (grey areas) are visible toward the top of the image where the view is through a short edge of the 3D volume.

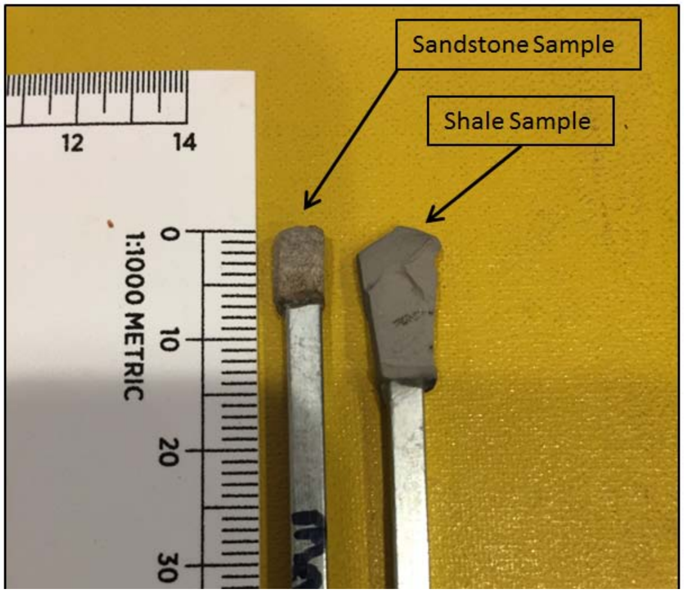

Figure C1-3. Cut or broken rock samples are attached to a metal rod before placing the sample into the CT scanner.

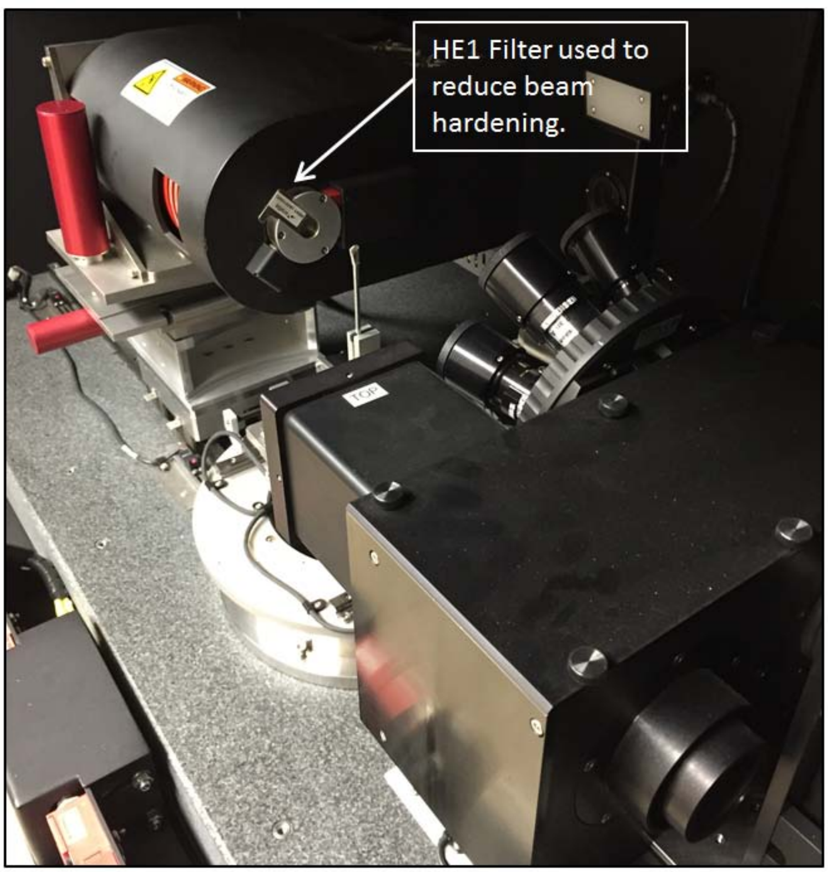

Figure C1-4. Rock sample attached to holder and placed between the source and detector within the CT scanner. In this image, a HE1 filter has been attached to the source opening.

Scanning consists of building a software-based 'recipe' that contains the procedure from which the machine will acquire a scan. The recipe has multiple sections including acquisition, camera, source, magnification, and references. Exact recipes require trial and error until the desired image has been attained. Critical controls are the source voltage and power, magnification of the detector, beginning and ending points for the scan, and how the images are to be reconstructed.

Setting the power and voltage of X-rays leaving the source determines how much penetration of the sample will occur and ultimately, how many X-ray will arrive at the detector. Too low a setting and no X-rays will penetrate the sample, too high a setting and the detector will be saturated causing artifacts in the images. Trial and error (many test scans) are required to identify a voltage that will provide a good source to signal ratio without creating image artifacts. Changes in materials properties, i.e., new rock types, require a new recipe to be developed.

C1.2. CT Results

To date, the majority of the time on this project was spent in developing recipes for shale samples. As specified above, exact power and voltage setting must be correctly determined to provide an image of high resolution for analysis. This process required several months of work by a geology MS student at SDSMT. A reality of CT scanning includes a paucity of information on exact techniques and recipes for shale samples. This is a response to the majority of shale research being proprietary within oil companies and although CT scan results are widely reported, the techniques utilized are not. Thus, we were forced to develop our own recipes for shale scanning and determining the correct combination of power and voltage was a time-consuming process. During this process, the two most common image artifacts resulting from power settings were ring and starburst effects. These features result within an image when X-rays generated by a high power setting encounter a high density material such as pyrite or barite and scatter instead of penetrate (Fig. C1-5). At the end of the experimentation period, recipes were developed for correct power and voltage settings for both shale (Fig. C1-6) and sandstone (Figures C1-1 and C1-2).

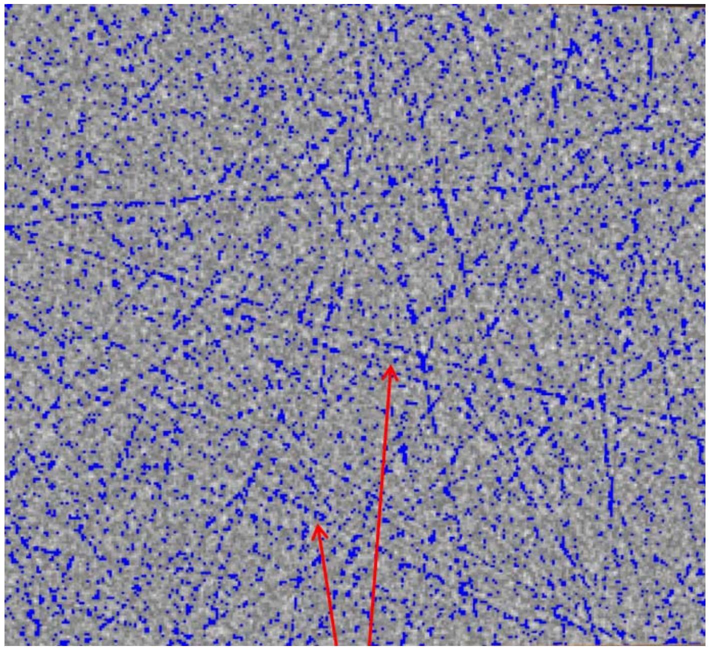

Figure C1-5. Starburst artifacts in shale samples caused by too high of energy X-rays striking higher density minerals such as pyrite and barite (red arrows). The streak pattern disrupts X-ray penetration and acquisition of quality scan images.

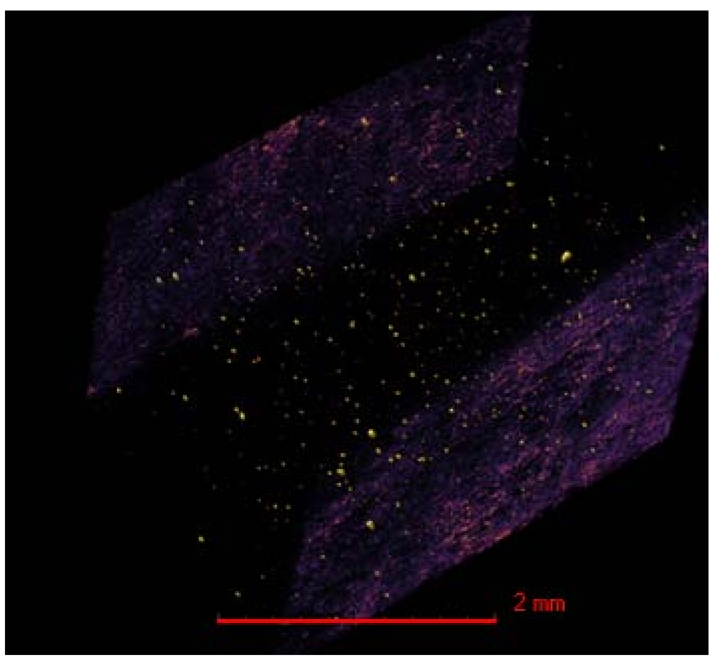

Figure C1-6. CT scan of shale with an appropriate power and voltage setting such that 3D imaging becomes possible. Here, the image contrast has been adjusted to remove all low density clay materials and to highlight the higher-density pyrite shown as the small golden spots. The red scale is 2000 μm, or 2 mm.

C2. SEM Scanning of Shale Core Materials from South Dakota

Scanning electron microscopy (SEM) produces high resolution imagery of surface topography (form) and chemical composition (mineral identification). It operates by focusing an electron beam generated by an internal electron source that is magnetically focused onto the surface of the specimen. The interaction between the electron beam and the sample produces signals that are processed to produce a two-dimensional raster image of the sample. This layout is demonstrated in Figure C2-1. SEM is operated under high vacuum and the sample is typically carbon or gold plated to produce electrical conductivity for electron beam interactions to occur.

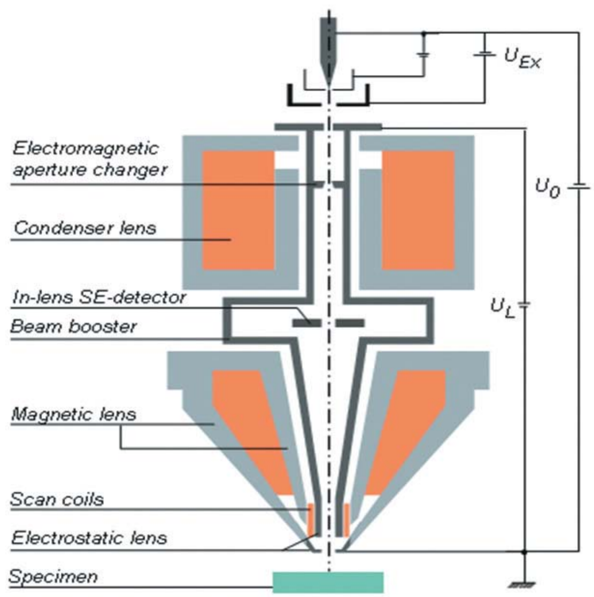

Figure C2-1. Schematic layout of SEM electron beam generation (modified from Huang et al., 2013). The electron beam is generated from a source and passed through an upper condenser lens that demagnetizes the beam. The beam then passes through a magnetic focusing lens that narrows the beam and intensifies the beam-sample interaction point.

Bombardment of the sample by the electron beam produces generated electrons that are derived from different parts of the sample. SE1 electrons come from very near the electron beam-sample interaction point and therefore carry high-resolution, surface-topology information. SE2 electrons are generated from deeper within the sample and are therefore lower-resolution topology but carry mineralogical data (Fig. C2-2). Both SE1 and SE2 electrons also produces a backscattered electrons, BSE1 and BSE2, respectively. BSE1 electrons provide compositional contrast and BSE2 electrons provide composition and crystalline structure data of the sample.

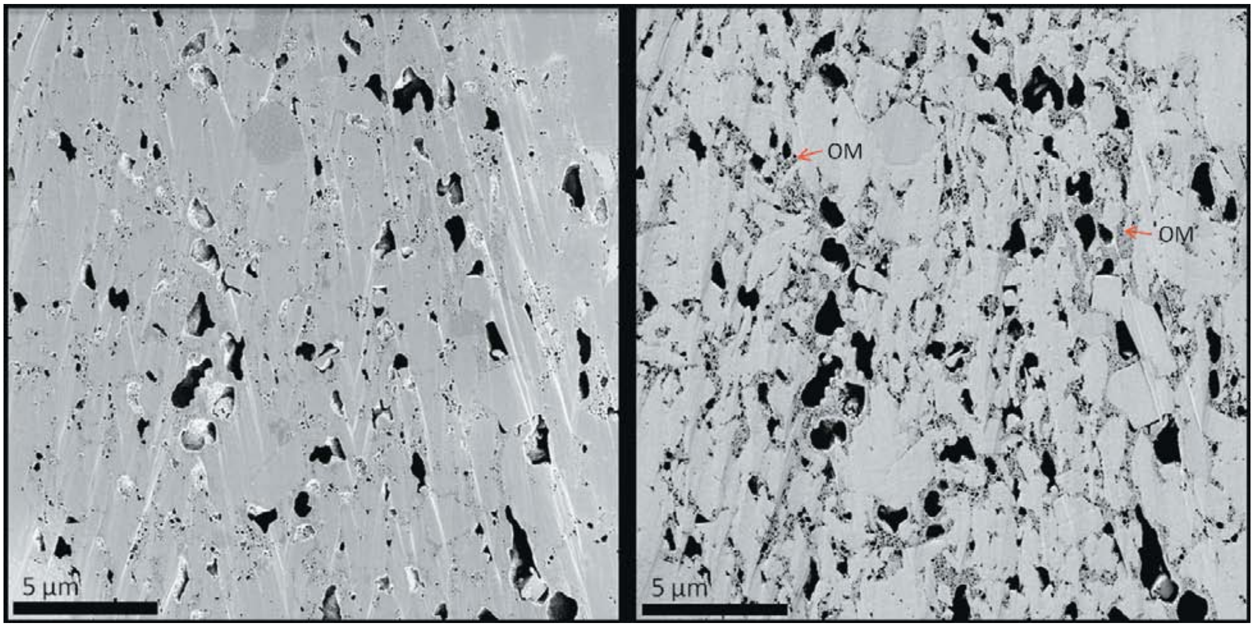

Figure C2-2. SE1 (left) and SE2 (right) imagery of a shale sample. SE1 imagery contains surface topology and other surface information such as pore spaces (black spaces). SE2 imagery is derived from deeper in the sample and provides mineralogical information not evident from SE1. Here, organic matter (OM) has been detected between shale particles and pore spaces (red arrows). Images are from Huang et al., 2013.

Samples from the Pierre shale core were analyzed using SEM to determine both surface topography and mineralogy. Figure C2-3 is a SE1 image of surface topology of a shale sample. The plate-like grain shape is obvious and the resulting inter-granular pore spaces are well defined. This image illustrates the fact that shales are typically high porosity rocks, i.e. they have a large voids-to-solids ratio but have low permeability or connectivity of the pores. Two barite crystals are also present in this sample (white arrows). No organic matter was identified. Figure C2-4 is from the same sample but contains measurements of pore sizes that range from sub-μm to over 10 μm wide.

Figure C2-5 is a high-resolution SE1 image that contains a fossil foraminifer that is ~140 μm long. This fossil displays excellent topographic information and appears to be three-dimensional in view. The shale plates above and below the foraminifera suggest bedding structures (white arrows) that undulate, which is common in fine-grained clay. Inside the foraminifer body are clusters of white crystals that are shown under higher magnification in Figure 5.6. These crystals are octahedral pyrite (FeS_2) that are 1 micron on edge and are perfectly formed and terminated.

Continued SEM imagery of the Pierre shale core will be performed to identify depositional setting, mineralogical variations, and to characterize pore size and distribution. Deformation of the shale structure will also be studied after mechanical testing of a sample.

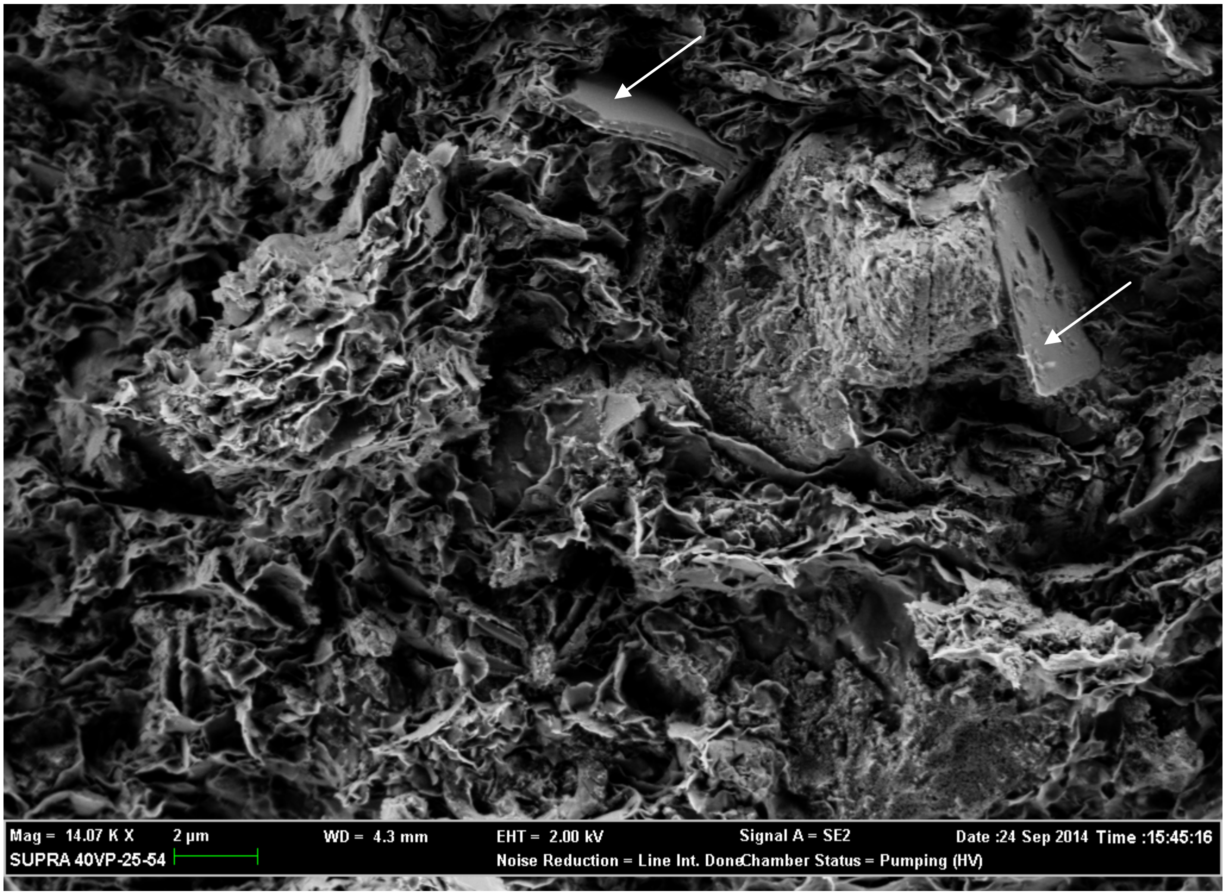

Figure B2-3. Pierre shale sample containing barite crystals. Green bar is 2 μm.

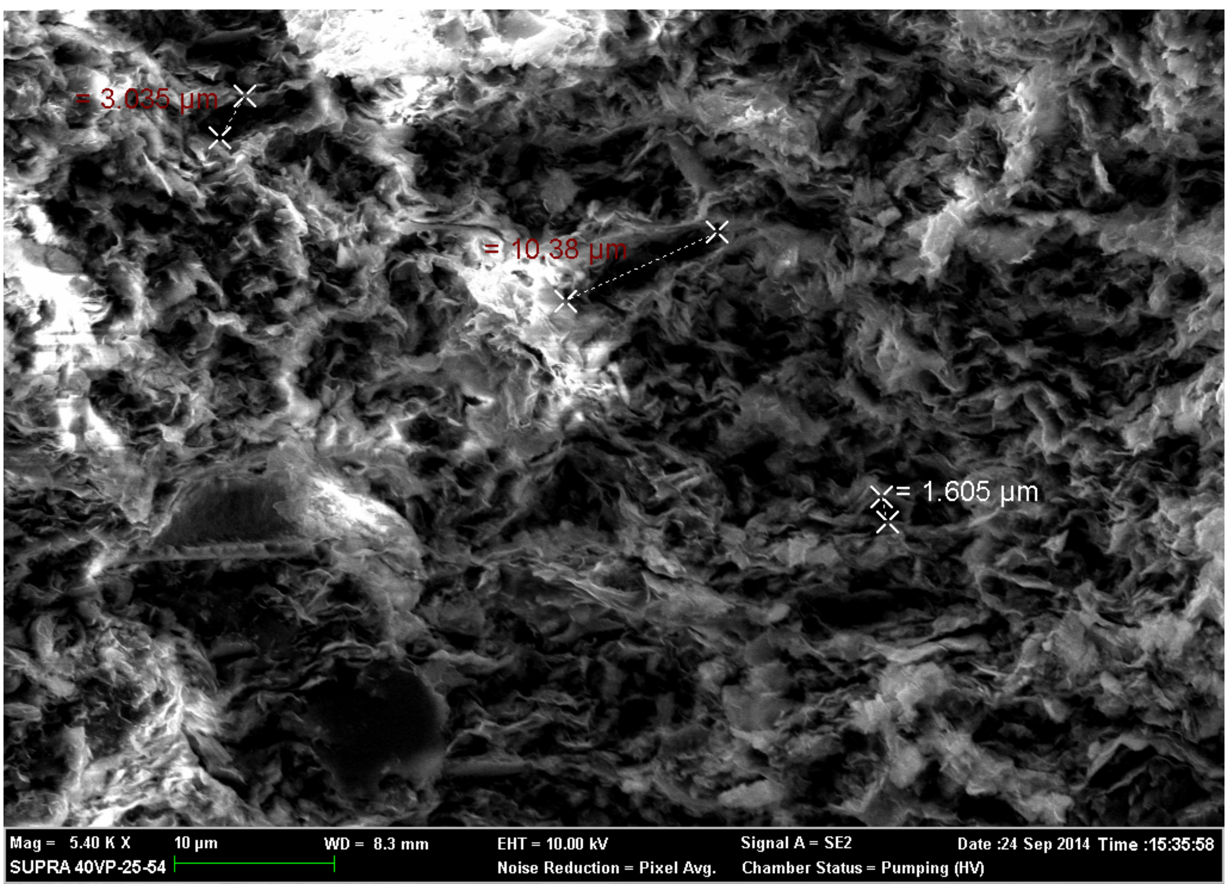

Figure B2-4. Pierre shale sample with measured pore spaces. Green bar is 10 μm.

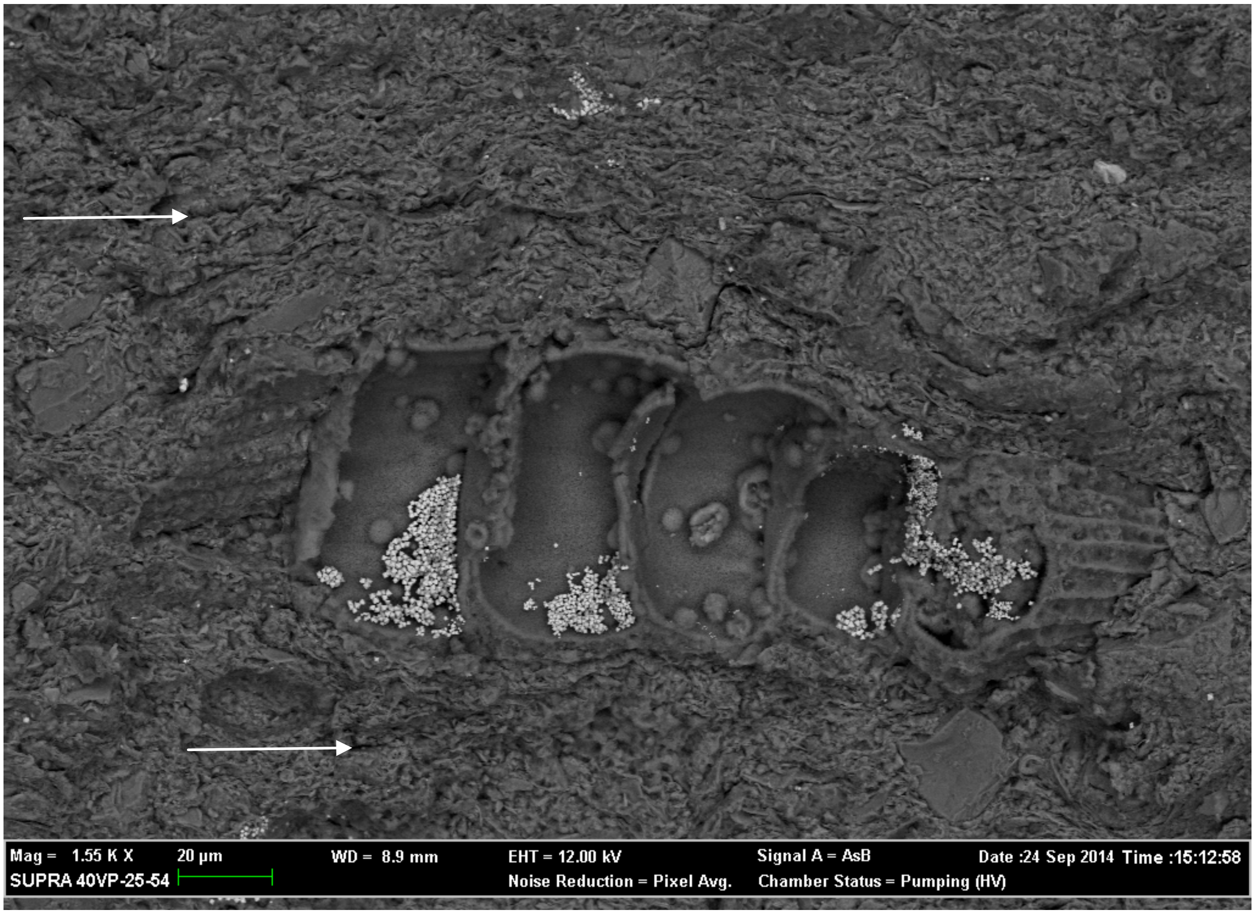

Figure B2-5. Pierre shale sample with foraminifera fossil. Green bar is 20 μm.

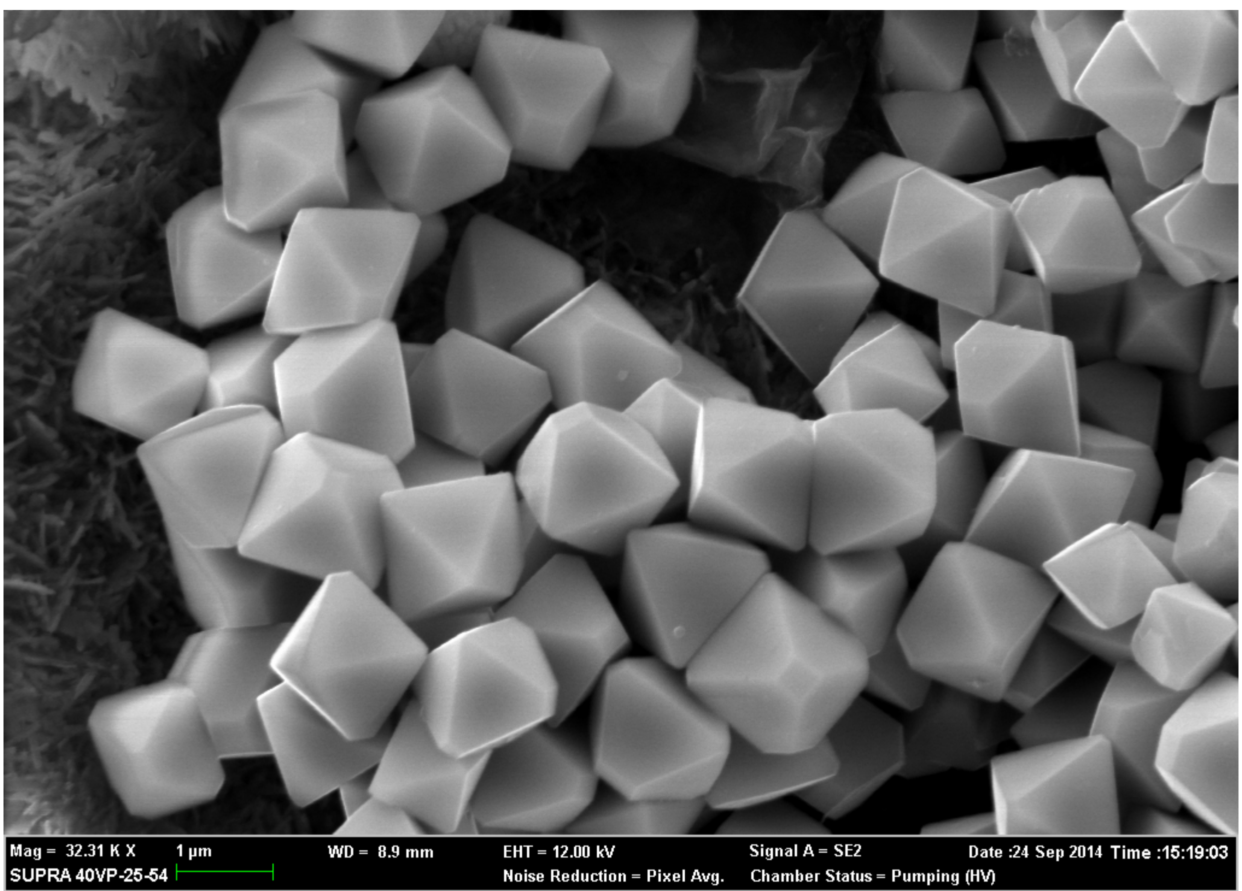

Figure B2-6. Pierre shale sample with pyrite crystals. Green bar is 1 μm.

References:

Huang, J., T. Cavanaugh, and B. Nur. 2013. An introduction to SEM operational principles and geologic applications for shale hydrocarbon reservoirs. In Camp et al. (eds.), *Electron Microscopy of Shale Hydrocarbon Reservoirs*. Memoir 102, American Association of Petroleum Geologists, 260p.

APPENDIX D Analysis of the Crow Creek Member of the Pierre Shale in Central South Dakota

D1. Introduction

The Crow Creek Member of the Pierre Shale was encountered during drilling of the Tree Dam core (Fig. D1-1) at a depth of 452 to 456 feet. This four foot interval of unconsolidated clay-rich coarse sand represents a marked change in deposition and lithology from marine shale below and above. The sandy stringer was loose in the core barrel and was not a standard competent core (Fig. D1-2). Stratigraphically, the Crow Creek lies unconformably above the Gregory Member and has been assigned to the lower-most DeGrey Member of the Pierre (Fig. D1-3).

Past research (Witzke et al., 1996; Anderson and Witzke, 1994) has attributed the Crow Creek to a depositional event resulting from a tsunami wave created by a bolide impact at the Manson Impact Structure in Iowa (Fig. D1-4). At the time of the impact roughly 74 million years ago, most of the interior of the North American continent was covered by the Western Interior Seaway (Izett et al., 1993). Normal marine deposition above and below the Crow Creek has been interrupted and the clay sand interval has been dated by Izett et al. (1993) as 74 million years old correlating to the time of the impact. Additionally, the Crow Creek thins to the west away from the Manson impact structure (Witzke et al., 1996).

D2. Objective:

The objective of this research project was to microscopically analyze samples of the Crow Creek to determine depositional properties and correlate the results to the published mineralogical data from the Manson Impact structure. If bolide evidence is determined, it will extend the known occurrence of impact debris about 150 km westward.

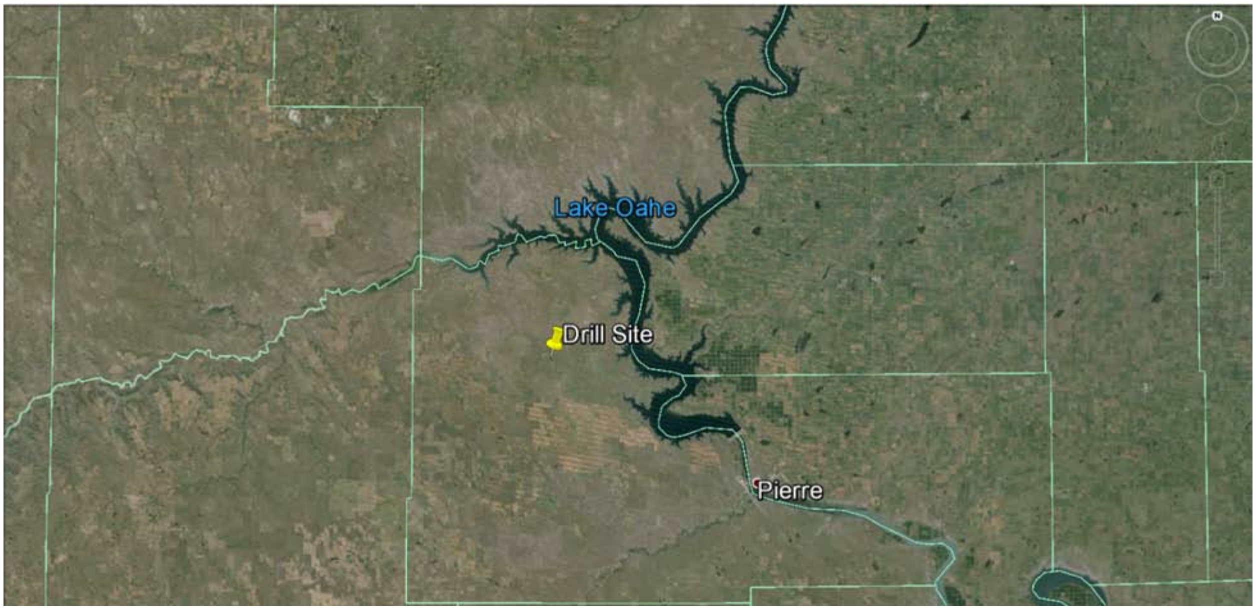

Figure D1-1. Drilling location for the Tree Dam core in South Dakota.

Figure D1-2. Part of the Tree Dam core containing the Crow Creek member. The material was a coarse sand in a clay matrix making the material sticky but unconsolidated.

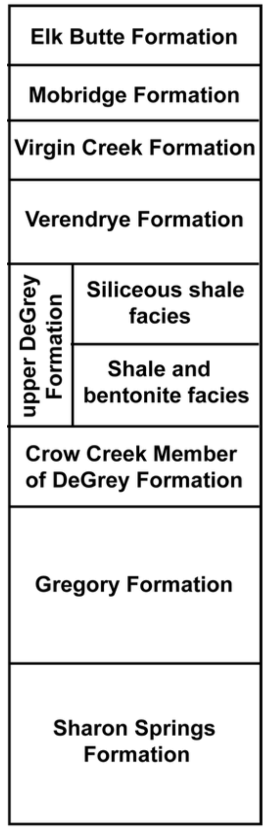

Figure D1-3. Stratigraphic column of the Pierre Shale formation showing the occurrence of the Crow Creek Member (Parris et al., 2007).

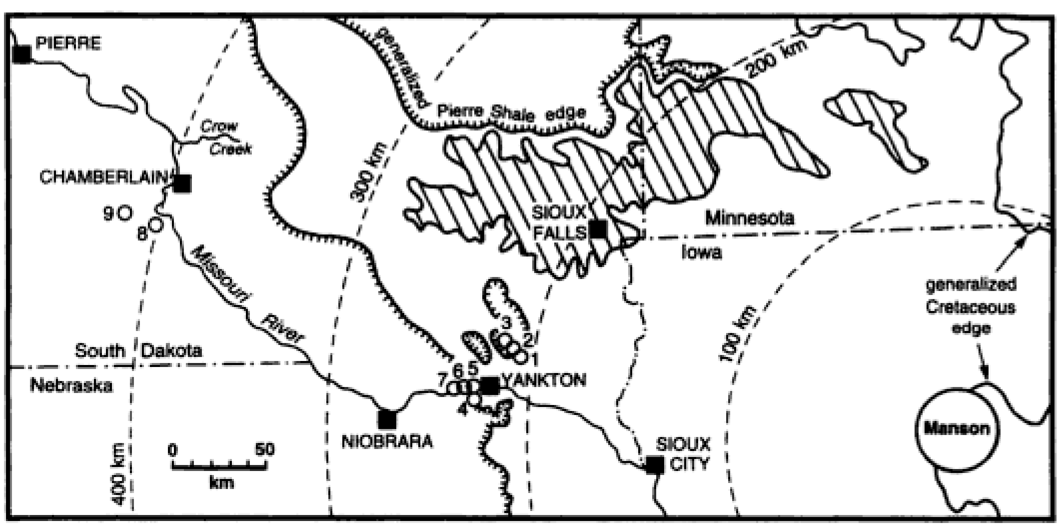

Figure D1-4. The Manson impact structure was centered at Manson, IA and debris resulting from the event has been previously detected as far west as Chamberlain, SD. The Tree Dam drilling site was ~600 km from the impact site and is located NW of Pierre, SD (not shown on this map from Witzke et al., 1996).

D3. Methods

Material from the drill core was separated into four samples, each representing a 1 foot interval. A small portion of each sample was washed to remove the clay and oven dried. All samples were sieved to determine grain size distributions. All samples were microscopically examined to determine grain shape and roundness and to determine if particular grain sizes contained specific minerals. Photo images were acquired throughout the process (Figures D3-1, D3-2).

Four grain-mount thin sections were prepared for each 1 foot interval and mineralogically examined under normal and cross polarized light to identify individual mineral grains. Grains showing possible planar deformation features (PDFs) were also identified. PDFs are considered diagnostic for minerals that have been altered by exposure to high shear stresses, such as the shock of impact from a bolide. Mineral grain identification was conducted on the upper most (452'-453') and lower most (455'-456') thin sections to provide percentage of mineral occurrence for comparison to published data from the Manson event.

Mathematical analysis for the ejecta blanket from the Manson event was also conducted using an empirical equation (Equ. D3-1) from Katongo et al. (2004) for other known sites within the state.

$$t = 0.14R^{0.74}\left(\frac{r}{R}\right)^{-3} \qquad \text{(D3-1)}$$

where:

R = radius of Manson impact structure (~18.5 km)
r = distance from Manson impact structure
t = thickness of the ejecta blanket

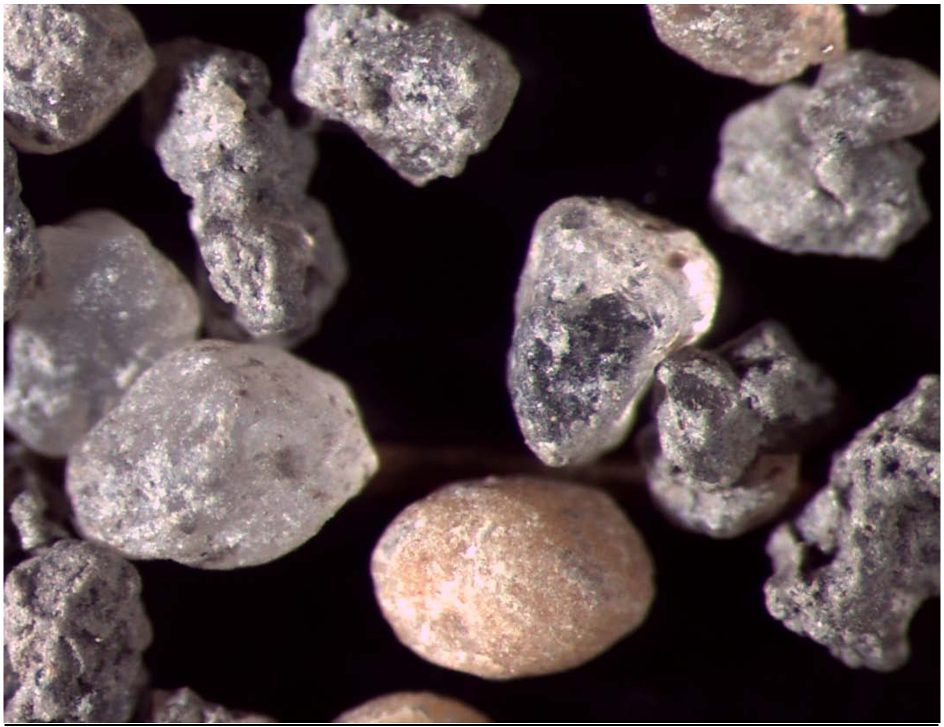

Figure D3-1. Portion of grains retained on the 0.595 mm sieve (No. 30 size) consists of quartz and rock fragments. Quartz grains were mostly subangular to subrounded clear crystalline quartz and fewer grains were rounded and frosted.

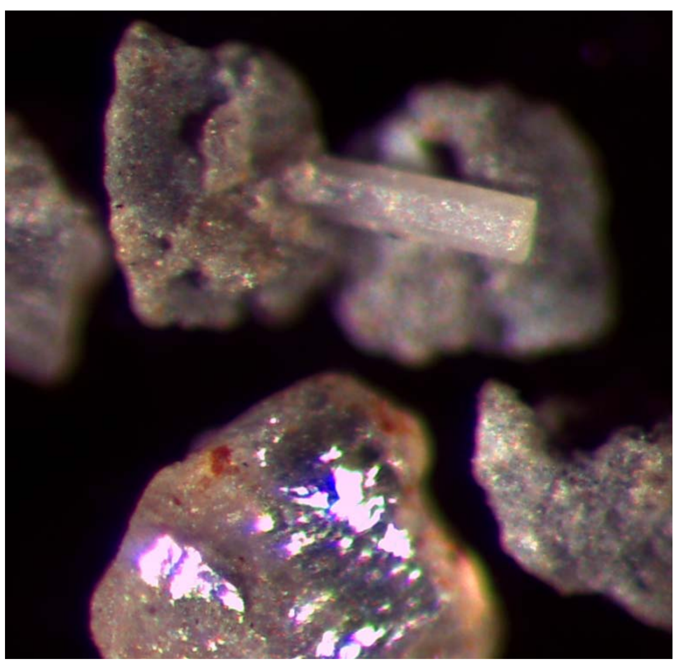

Figure D3-2. An authigenic hexagonal quartz crystal.

D4. Results

1. Sieved Samples

Sieve results were mostly consistent between the various depths and 31 percent of the grains in the Crow Creek were retained on the No 40 sieve, or 400 microns (Table D3-1). Sample #23 (455' to 456'), however, contained significantly higher concentrations for the coarsest grains, 1190 and >1190 micron sizes and were 27.8 percent and 28 percent, respectively. The higher concentration in these large grain sizes was most likely due to the inclusion of pieces of the underlying Gregory Member in the core section.

Table D3-1. Percent weight values of grain sizes (microns) for individual samples (1 foot intervals) and average for the entire 4 foot thickness of the Crow Creek.

Size (microns)	452'	453'	454'	455'	Total
			Weight %		
>1190	0.93	5.09	0.54	27.90	8.86
1190	5.72	9.26	8.31	28.56	12.98
841	10.20	11.70	15.15	8.29	10.97
595	9.97	13.43	16.62	6.79	11.19
400	52.32	25.43	28.28	12.35	31.07
250	11.44	19.53	19.84	9.43	14.40
125	5.02	8.04	6.30	3.68	5.63
63	2.40	3.87	2.68	1.70	2.62
Pan	2.01	3.66	2.28	1.32	2.28

Microscopic examination of sieve samples from the No 30, 60, and 230 screens revealed that grains ranged from subrounded to subangular and very few grains were angular in shape. These samples contained quartz grains that were both frosted and clear, where the frosted grains were typically more rounded (Fig. D4-1). Witzke et al. (1996) determined that quartz grains dominated the Crow Creek Member to the west of the impact site and frosted grains were present. There were also a few distinguished grains of red quartzite (Sioux quartzite?) scattered throughout the Crow Creek.

Figure D4-1. A typical red quartzite grain most of which were subrounded to rounded. Source was unknown but considered to be Sioux quartzite.

2. Thin-sections

The thin-section analysis provided key information regarding the mineralogical makeup of the Crow Creek at the Tree Dam site. Cross-polarized light was used to identify minerals. Results are contained in Table D3-2. The dominant mineral was monocrystalline quartz, comprising 60 percent of the total grains identified, whereas the remainder was 11 percent polycrystalline quartz, feldspar 11 percent, microcline feldspar four percent, and other minerals in general 14 percent. These data are consistent with mineralogical data from other Crow Creek localities (Witzke et al., 1996).

Table D3-2. Grain identifications from thin-sections using cross-polarized light.

Mineral	Grain Count	Percent
Quartz	148	60
Polycrystalline Quartz	27	11
Microcline PDF	1	0.4
Microcline	11	4
Other Feldspars	26	11
Other Minerals	34	14

3. Shock Grains

A key element of this research was to determine if shocked minerals were present in the Crow Creek at this location. Shocked minerals display internal deformations in the crystal lattice called planar deformation features (PDFs). Typical minerals having PDF structures include quartz and lesser occurrences in mica, feldspar, and sandstone. Katongo et al. (2004) reported the occurrence of shocked quartz grains in the Gregory core obtained near Chamberlain, SD. These were extremely rare and limited to the basal unit of the Crow Creek (Fig. D4-2). To date, no indications of this type of shocked quartz have been discovered from the Tree-Dam core.

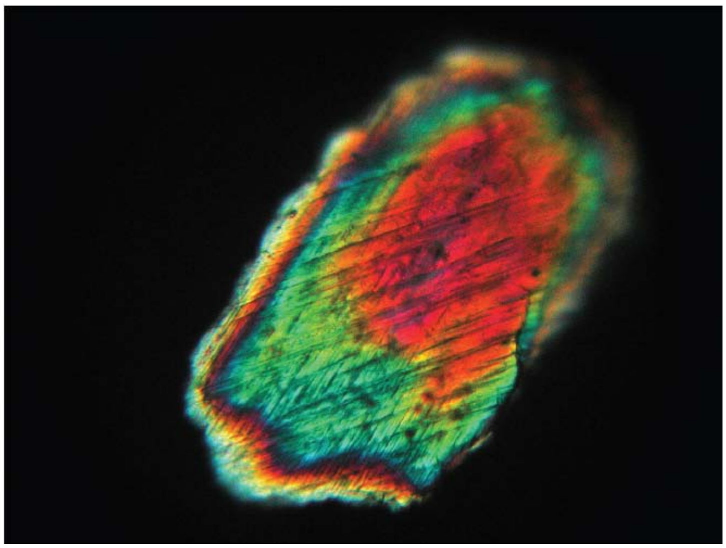

Figure D4-2. Shocked quartz grain from the Gregory core near Chamberlain, SD (from Katongo et al., 2004). Note the black lines, lines of internal crystal deformation due to high energy impact, or shock.

Other PDF structures in quartz include polycrystalline multiple extinctions and kink bands. These PDFs are reported from most bolide impact sites including the Azuara impact structure and the Rubielos de la Cerida impact basin, both in Spain. Witzke et al. (1996) suggested that polycrystalline quartz (mottled multiple extinctions) occurrences indicate unshocked ejecta. Figure D4-3 contains identified mottled extinctions from Spain and those grains observed from the Crow Creek. The occurrences are identical. Figure D4-4 contains kink band deformations in quartz from Spain and the Crow Creek. Again, the features are identical. If the presence of polycrystalline quartz and kink bands in quartz are caused by shock impact grains, impact evidence has been detected in this core with ~11 percent of the grains being polycrystalline quartz and kink bands being observed in numerous grains.

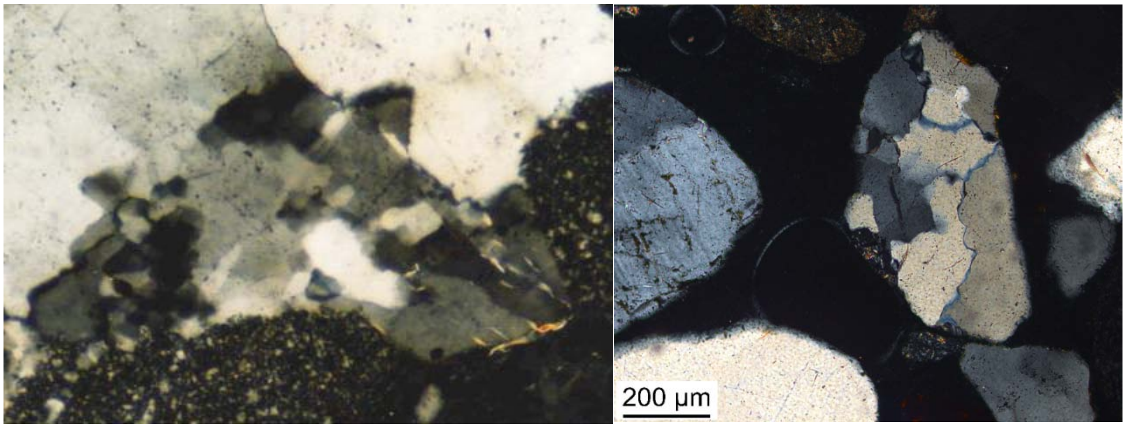

Figure D4-3. Mottled polycrystalline quartz from Spain (left) and the Tree Dam site (right) in South Dakota. Both display multiple extinctions.

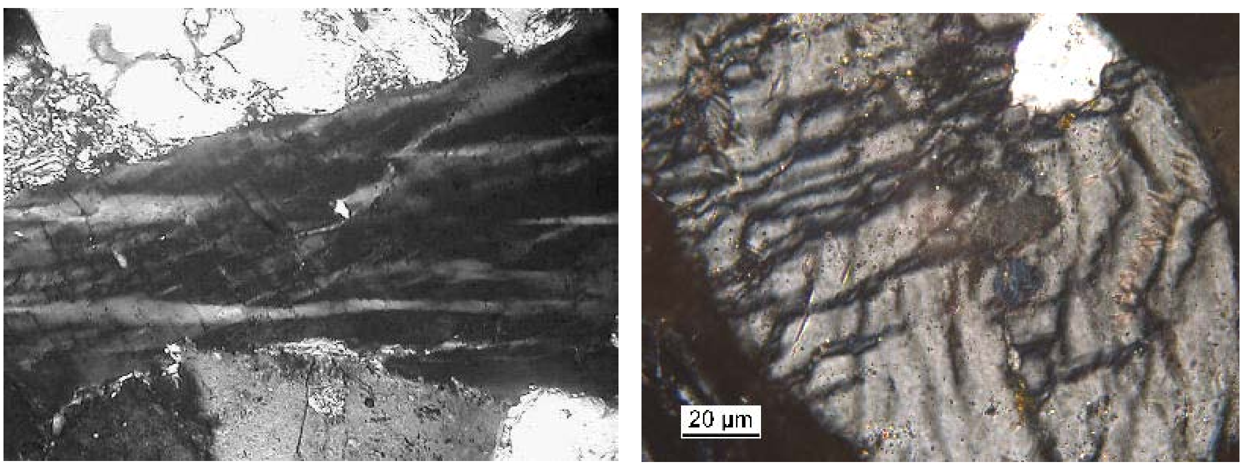

Figure D4-4. Kink bands in quartz grains from Spain (left) and the Tree Dam core (right) in South Dakota.

Sandstone PDFs occur as swarms of linear deformation features in a single grain. Figure D-5 contains shocked sandstone from Sudan in Canada and the Tree Dam core. These features are identical and the shocked sandstone deformations were observed in several grains.

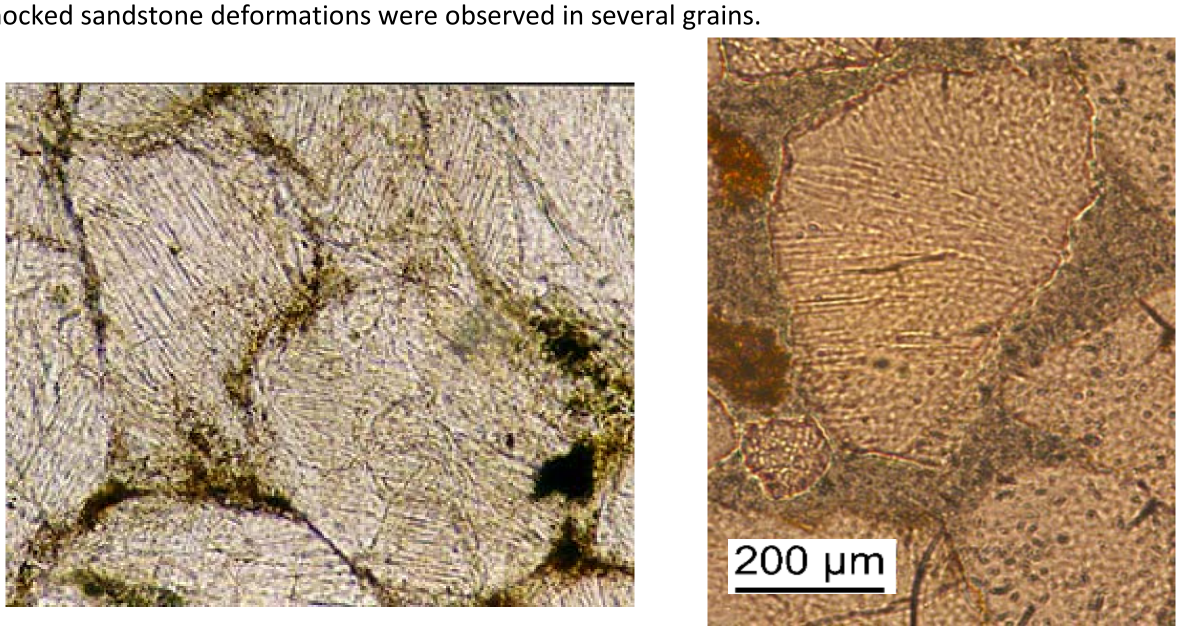

Figure D4-5. Shocked sandstone from the Sudan crater in Canada (left) and from the Tree Dam site (right) in South Dakota.

A single grain of microcline feldspar possessing PDFs was observed in the thin-section from the 452'-453' sample (Fig. D4-6). The discontinuation of the twinning throughout the grain suggests rapid and high stress-induced deformation. Others have noted the presence of shocked feldspars within the Crow Creek at other localities (Witzke et. al, 1996; Katongo et al., 2004). The single grain of shocked microcline accounted for less than 1 percent of the total minerals (Table D3-2). Izett et al. (1998) reported the presence of microcline to be exclusive of Manson impact debris.

4. Mathematical Analysis

Bolide impacts produce ejected materials that travel into the atmosphere and settles into deposits on the land surface or seafloor. The resulting deposit is referred to as an ejecta blanket (Katongo et al., 2004). The thickness of the ejecta blanket is proportional to the distance from the site of the impact and can be calculated using equation 1. The thickness of the ejecta blanket has been referred to as the 'basal' unit of the Crow Creek Member (Katongo et al., 2004). A value for the radius of the Manson impact structure of 11.5 miles was obtained by Katongo et al. (2004). The distance from the Tree Dam Site to the Manson impact structure was obtained using Google Earth and was 345 miles. The resulting value of ~0.5 inch for this distance indicated that atmospheric settling would have potentially deposited a thin layer of ejecta on the shallow sea floor. This contradicts with the ~4 foot thick Crow Creek section at the Tree Dam site. However, the resulting tsunami wave generated by the ~2×10^{21} Joules of released energy (Varricchio et al., 2010) by the impact would have stirred up the seafloor and transported additional debris from closer to the impact westward across the sea. The result appears to be the ~4 foot thick sandy debris layer encountered in the Tree Dam hole. The material derived from this study constitutes furthest westward extent of the Manson Impact fallout, although whether it was derived as an airfall or as a tsunami deposit is still undetermined. The presence of the sandy deposit at the Tree Dam site (near Pierre) and not at Presho where the Crow Creek consists of marl and siltstone is also worthy of note and may indicate paleotopography on the seafloor that led to a modification of the original deposit.

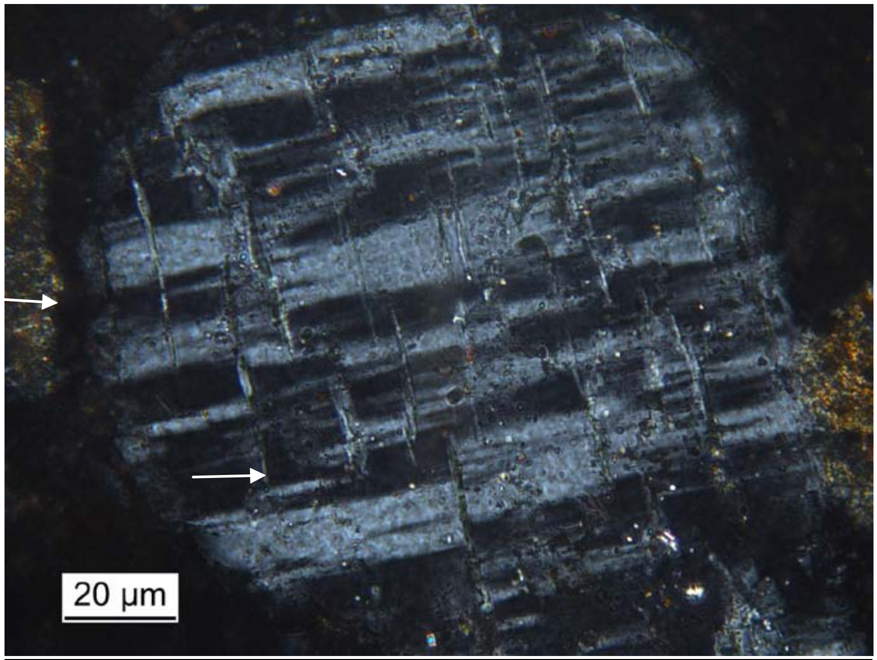

Figure D-6. Shocked microcline feldspar from the Tree Dam site which displays planar deformation features. Notice the offsetting of twinning within the crystal, which is more apparent in the lower portion.

References:

Anderson, R.R. and B.J. Witzke. 1994. The terminal cretaceous Manson impact structure in North-central Iowa: A window into the Late Cretaceous history of the eastern margin of the Western Cretaceous Seaway. Geological Society of America Special Papers, 287:197-210.

Witzke, B.J., R.H. Hammond, and R.R. Anderson. 1996. Deposition of the Crow Creek Member, Campanian, South Dakota and Nebraska. Geological Society of America Special Papers, 302:433-456.

Izett, G.A., W.A. Cobban, J.D. Obradovich, and M.J. Kunk. 1993. The Manson impact structure: 40Ar/39Ar age and its distal impact ejecta in the Pierre Shale in southeastern South Dakota. Science, 262:729-732.

Parris, D. C., B.S. Grandstaff, and W.B. Gallagher. 2007. Fossil fish from the Pierre Shale Group (Late Cretaceous): Clarifying the biostratigraphic record. Geological Society of America Special Papers, 427:99-109.

Katongo, C., C. Koeberl, B.J. Witzke, R.H. Hammond, and R.R. Anderson. 2004. Geochemistry and shock petrography of the Crow Creek Member, South Dakota, USA: ejecta from the 74-Ma impact structure. Meteoritics & Planetary Science, p31-51.

Izett, G.A., W.A. Cobban, G.B. Dalrymple, and J.D. Obradovich. 40Ar/39Ar age of the Manson impact structure, Iowa, and correlative impact ejecta in the Crow Creek Member of the Pierre Shale

(Upper Cretaceous), South Dakota and Nebraska. Geological Society of America Bulletin, 110:361-376.

Varricchio, D.J., C. Koeberl, R.F. Raven, W.S. Wolbach, W.C. Elsik, and D.P. Miggins. 2010. Tracing the Manson impact event across the Western Interior Cretaceous Seaway. Geological Society of America Special Papers, 287:197-210.

APPENDIX E Micropaleontology

E1. Approach

The methodology used in this study was adapted from that of two previous large-scale analyses of the Pierre Shale. Mello (1969) sampled the Pierre Shale, as well as the Fox Hills Formation, in 5’9” intervals and utilized a lab procedure that called for boiling approximately 110g of sediment in a solution of washing soda (sodium carbonate) and water until the sample was fully dissociated. This was followed by wet-sieving of the sample. After wet-sieving, the sample was allowed to sit and dry before being sieved again. In this project, coring at Presho #1 was performed through the Pierre Shale to a depth of approximately 549 feet with each core being taken at proposed five-foot intervals. Samples to be processed and examined for this study were taken from the shoe sample of each core and were chosen by taking every other specimen in an attempt to maintain 10-foot intervals. The estimated intervals, as well as the actual depth taken from the coring logs, for each sample are included in Figure E1-1 for this study. In addition to the standard-interval sampling, other samples were chosen based on lithological characteristics that indicated inclusion of those samples may provide further information that would aid in paleontological distinctions between units. Following sample selection, specimens were processed for boiling in a manner similar to that of Mello (1969); however, as not all of the samples utilized for this study had enough material to take approximately 100g, it was determined that if it was not possible to take 100g of material, approximately 25-50 percent of material retrieved from the shoe sample would be used in the study. Using this adapted procedure, specimens to be boiled ranged from 10g – 130g. Once the specimens were processed into smaller fragments, they were allowed to boil for anywhere between 1-2 hours until they appeared to be fully dissociated. Following boiling, the specimens were then wet-sieved over a series of sieves (250µm, 150µm, 105µm, 74µm, 53µm, 36µm) and allowed to dry for approximately 5 days. Specimens were then spread over a tray and scanned using a binocular microscope. Observed microfossils were then removed using an 18/0 paintbrush and placed onto gridded slides which were pre-coated with a Tragacanth gum mixture. Identifications of recovered microfossils were based on Mello (1969; 1971) and Hart, et al (1989).

E2. Results

The majority of microfossils were observed in the 250µm, 150µm, and 105µm fractions. While specimens were observed in the 74µm fractions, removal of these specimens from the sediment samples proved difficult with the materials on hand and a decision was made that fractions below 105µm were to be left to be sampled at a later date because of time constraints. A list of specimens identified in each core is included in the attached Figure E1-1 for this section. A cursory examination of the specimens identified shows no continuous occurrence of microfossil taxa or distinct boundaries that could correlate to known members of the Pierre Shale. A full listing of identified taxa with their presence in the core, including the depths at which they were observed, is presented in an attached Figure E1-1. Taxon presence is indicated by an infilled black spot.

E3. Discussion

The micropaleontology portion of this project was undertaken with the aim of attempting to constrain the various members of the Pierre Shale within the core recovered from the drill sites. The Pierre Shale is often divided into several members, which are distinguished by features visible in outcrop, but which may not be readily apparent in the core samples recovered. Due to the abundance of microfossils throughout marine sediments, it was believed that it could be possible to utilize biostratigraphic zonation in order to locate possible boundaries within the core that would reflect changes within the depositional environment of each member. Such biostratigraphic zonations have been compiled for the Cretaceous Period previously (Bralower, et al, 1995) and were referenced for use in this work.

Bralower, et al (1995) integrated results using planktonic foraminifers, nannofossils, and calpionellids to construct their biostratigraphic scheme, which resulted in 73 integrated biostratigraphic zonations providing a much higher resolution than had previously been appreciated. These zonations span the Cretaceous from the start of the Berriasian (145 ma) to the end of the latest Maastrichtian (65 ma). The Pierre Shale spans a period of time of approximately 15.1 ma from the Campanian to the mid Maastrichtian. The scale composed by Bralower, et al (1995) shows approximately 10 biostratigraphic zonations in this time period. However, no zonal scheme will be globally applicable because of environmental differences between regions, especially as temperatures gradients in the local environment would have strongly influenced the geographic ranges of these taxa. This implies that the correlation of Western Interior zones to the European zones would be indirect because of the different assemblages native to each region. Bralower, et al (1995) attempted to account for this by sampling 14 localities in the Western Interior and tying the radiometric dates obtained from these samples to those obtained from European samples. These attempts only had minor success as only half of the localities were able to be dated, and only 10 percent of the total samples processed preserved usable material. This amount of material still allowed for correlation of Western Interior sediments to their integrated scale. Despite this correlation, it is important to note that the zonations of Bralower, et al (1995) do not correspond directly with the various members of the Pierre Shale. The Pierre Shale was deposited over a large area in North America leading to differing depositional conditions throughout the geographic expanse of the formation, as well as throughout the depositional time of the formation, leading to different stratigraphic profiles between and within states (Gill and Cobban, 1965; Mello, 1971; Petsch, 1942). As such, the Pierre Shale can be subdivided into anywhere from two to eleven members, depending on where you observe the formation in outcrop. In central South Dakota where the coring for this project was performed, the Pierre Shale is divided into 8 members. This would conceivably allow for the direct correlation of the members of the Pierre Shale at the Presho core site area to the integrated zones of Bralower, et al (1995), however, none of the taxa noted as distinctive to their boundaries were observed in the samples processed from the Presho locality.

Comparisons were made to other biostratigraphic studies performed in similar localities to the site of drilling. Johnson (1961) allowed for correlation of the Gregory Member to the Gulf series from the southern United States, while Lange (1962) examined the biostratigraphy of the Verendrye Member and provided a rough biostratigraphic zonation for the Pierre Shale. Again, exact correlation of taxa between these studies and those recovered from the coring project was limited. Of the nine zones noted in Lange (1962), taxa that corresponded to only three of the zones were recovered, and their appearance did not appear as indicated in those zonations. Lange (1962) does provide a diagram showing the stratigraphic distribution of dominant foraminifera between the sections studied within the Verendrye Member which provides some insight on the results obtained in this study. In this diagram, the distribution of the various forms is non-uniform throughout the formation. This matches the condition observed in this locality very closely wherein many of the forms observed show variable ranges, often disappearing and then reappearing again.

This fluctuation in faunal composition could be a true reflection of the conditions of the Western Interior Seaway at this point in time, however the presence and absence of taxa in the samples observed could also be a product of diagenetic processes during preservation where calcareous fossils of this nature may have been lost because of dissolution both prior to, and following, final burial. Another feature of note is the fluctuating presence of more characteristically southern taxa in the samples examined. As stated above, the local environment would have had an impact on the geographic range of taxa that could possibly be preserved in the basin. Warmer temperatures would allow for a range extension of more southern taxa into the north while shifts to cooler temperatures would allow for the range extension of northern taxa into the south. Similar faunal-climate interactions have been observed in contemporaneous terrestrial localities (Larson, et al, 2010). Despite the absence of distinct boundaries, the observed taxa support the existence of a diverse, constantly changing assemblage in the interval observed by this study.

E4. Future Directions

Future directions for the material recovered in this project and for the work started in this project would be to conduct a further review of the faunal information recovered from the Presho #1 drill site, as well as verifying the validity of the identifications made for the recovered specimens with other paleontologists more familiar with Late Cretaceous foraminifera. Additionally, it would be beneficial to process the shoe samples obtained from the Presho #2 drill site using the same methods employed to study the specimens from Presho #1. In doing this, it may be possible to observe any similarities or overlap between the two drill sites that would permit further correlation or identification of faunas that may represent a given member of the Pierre Shale. In order to constrain the biostratigraphy of the Pierre Shale on a similar level to that of the European zones, it would first be necessary to attempt a large scale stratigraphic correlation of the various recognized members of the Pierre Shale that would be tied to radiometric dating. The initial step in an undertaking of this nature would be to initiate coring projects similar to this one in other areas where the Pierre Shale is known to exist in the subsurface. The coring projects would then produce a continuous record of the lithology of the Pierre Shale at various locations throughout the original depositional basin. Sedimentological analysis of the samples recovered would provide information on both the depositional environment of each portion of the Pierre Shale, as well as on the relationship of each section of the Pierre Shale to other sections throughout the extent of the Western Interior Seaway. Correlations produced in the sedimentological analysis would then provide a framework upon which further micropaleontological investigations could be performed. Due to the continuous sampling during coring, this would not only permit sampling near the same radiometrically dated points throughout the cores to provide a detailed comparison of the microfauna throughout the Western Interior Seaway at a given time, but would also allow for comparisons in terms of faunal changes relative to environmental pressures through time. Once a sufficient dataset has been compiled from various coring projects, it will then be possible to provide a detailed analysis of the biostratigraphy of the Pierre Shale including information that could allow for correlation with larger integrated biostratigraphic scales.

Figure E-1 Microfossil Taxonomic Occurrences (Depth - ft. from surface)

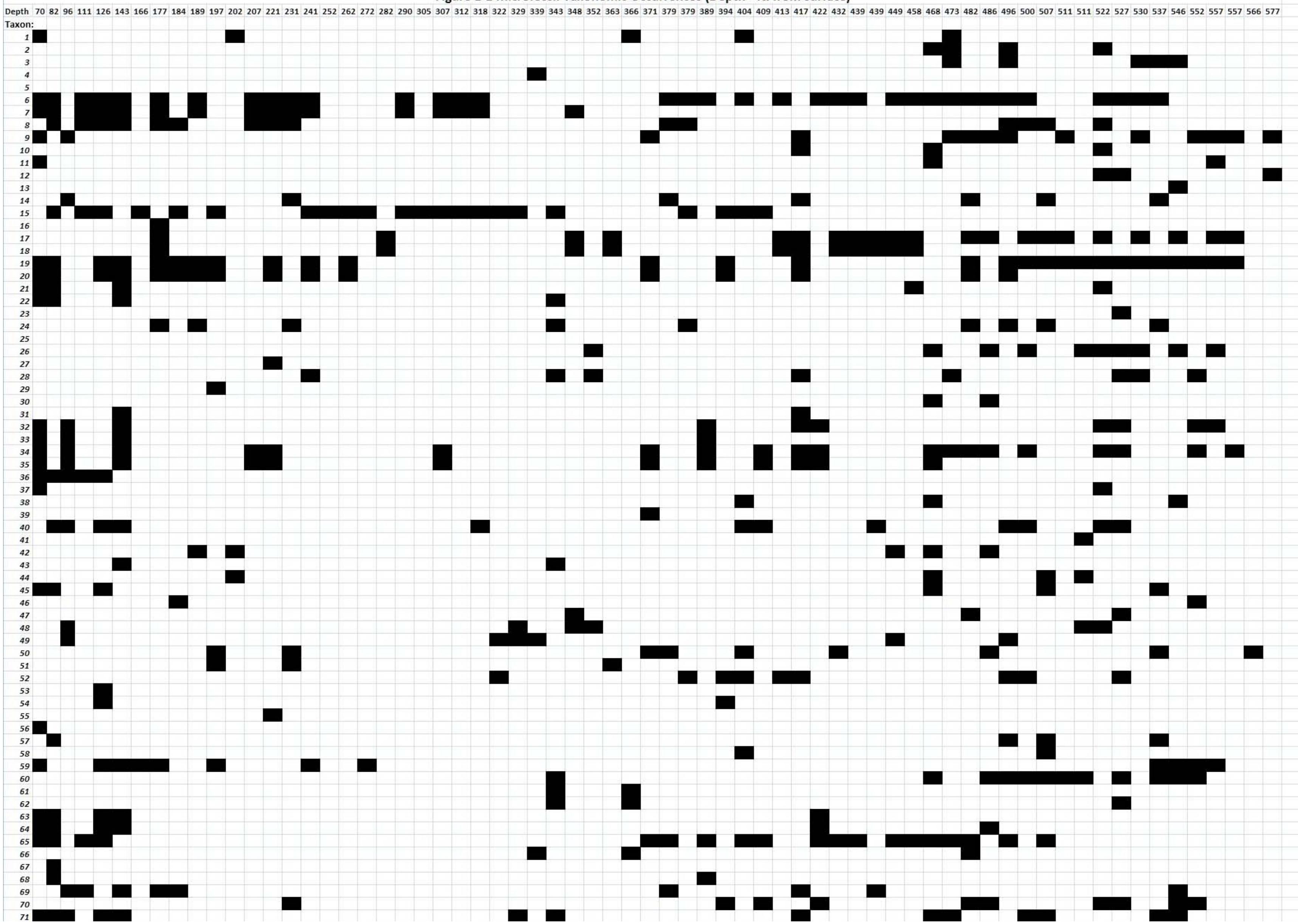

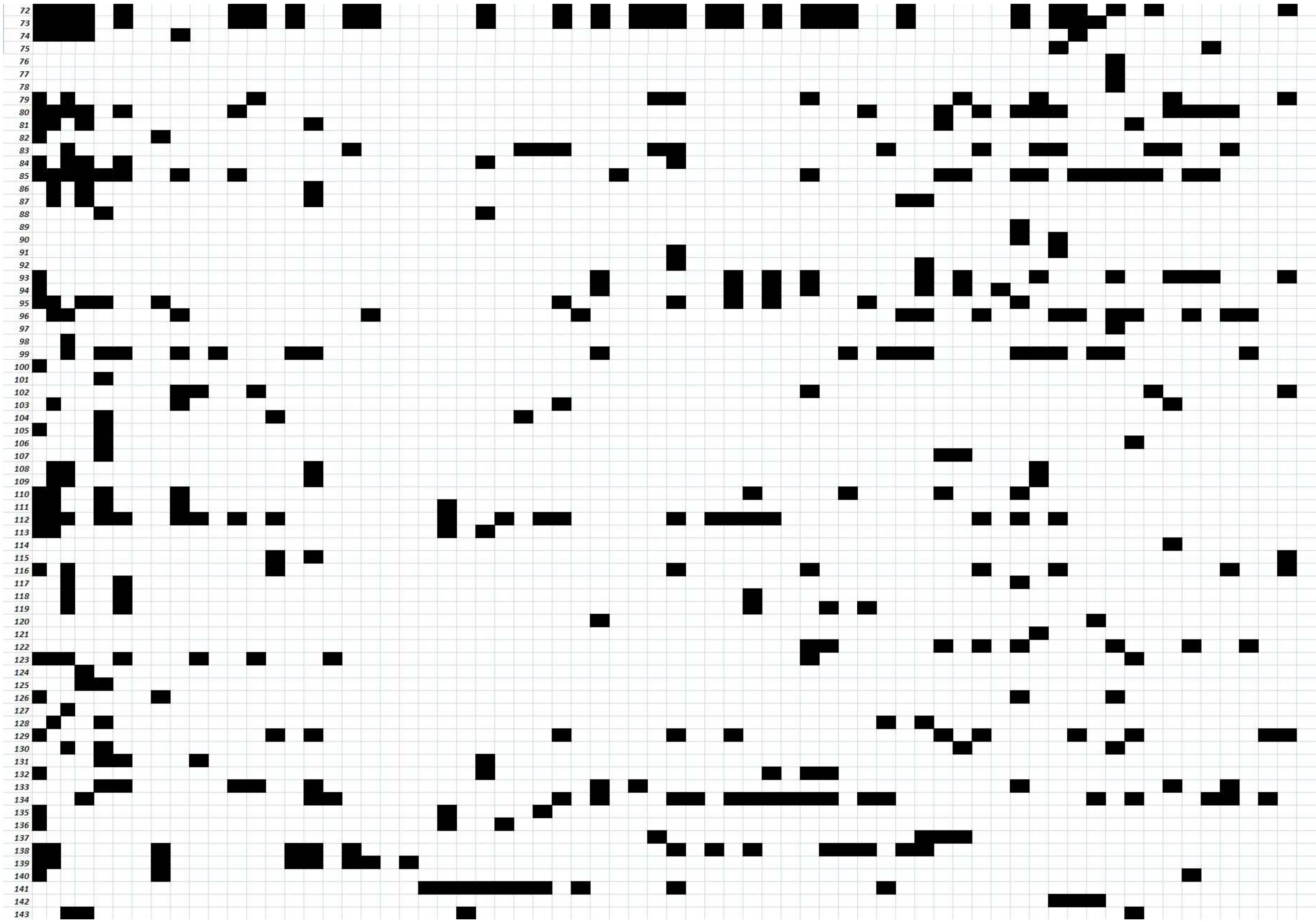
72
73
74
75
76
77
78
79
80
81
82
83
84
85
86
87
88
89
90
91
92
93
94
95
96
97
98
99
100
101
102
103
104
105
106
107
108
109
110
111
112
113
114
115
116
117
118
119
120
121
122
123
124
125
126
127
128
129
130
131
132
133
134
135
136
137
138
139
140
141
142
143

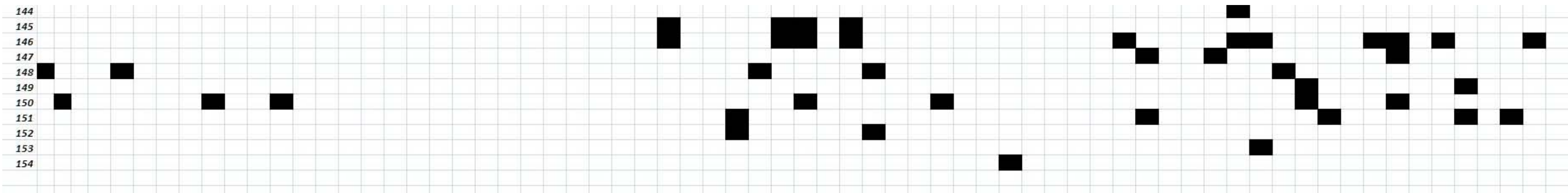
144
145
146
147
148
149
150
151
152
153
154

Key	Taxa	Key	Taxa	Key	Taxa
1	*"Discorbis" quadrilobus*	31	*Cibicides harperi*	61	*Globigerinelloides prairiehillensis* / Biglobigerinella biforaminata
2	*? Buliminella carseyae*	32	*Cibicides mobridgensis*	62	*Globigerinelloides sp.*
3	*Alabamina australis*	33	*Cibicides naranjoensis*	63	*Globulina lacrima*
4	*Alabamina sp. / Trochammina sp. ?*	34	*Cibicides sp.*	64	*Globotruncana sp.*
5	*Ammobaculites coprolithiformis*	35	*Cibicides sp. 2*	65	*Glomospira charoides*
6	*Ammodiscus cretaceus*	36	*Cibicides subcarinatus*	66	*Glomospirella inconstans*
7	*Ammodiscus sp. / Glomospirella sp.*	37	*Cibicidoides sp.*	67	*Guttulina trigonula*
8	*Anomalinoides minuta*	38	*Clavulinoides trilaterus*	68	*Gyroidina comma*
9	*Anomalinoides sp.*	39	*Colomia sp.*	69	*Gyroidina depressa*
10	*Anomalinoides pinguis*	40	*Dentalina sp.*	70	*Gyroidina girardana*
11	*Astacolus dissonus*	41	*Dentalina basiplanata*	71	*Gyroidina globosa*
12	*Astacolus narvarroanus*	42	*Dentalina catenula*	72	*Gyroidina sp.*
13	*Astacolus rectus*	43	*Dentalina consobrina*	73	*Gyroidina sp. / Hoeglundina sp.*
14	*Astacolus sp.*	44	*Dentalina gracilis?*	74	*Haplophragmoides bonanzaensis*
15	*Bathysiphon brosgei*	45	*Dentalina legumen*	75	*Haplophragmoides excavata*
16	*Bathysiphon vitta*	46	*Dentalina niobrarensis*	76	*Haplophragmoides rota*
17	*Bathysiphon sp.*	47	*Dentalina pertinens*	77	*Haplophragmoides sp. 1*
18	*Bathysiphon sp.2*	48	*Dentalina solvata*	78	*Haplophragmoides sp. 2*
19	*Biglobigerinella biforaminata*	49	*Dictyomitra multicostata*	79	*Haplophragmoides sp. ?*
20	*Biglobigerinella sp. ?*	50	*Dorothia smokyensis*	80	*Heterohelix globulosa*
21	*Bolivina decurrens*	51	*Dorothia sp.? / Gaudryina sp.?*	81	*Heterohelix pulchra*
22	*Bolivina sp.*	52	*Epistomina ornata*	82	*Heterohelix sp.*
23	*Bolivinopsis rosula?*	53	*Frondicularia watersi*	83	*Hoeglundina sp.*
24	*Bulimina sp.*	54	*Gavelinella sp.*	84	*Hoeglundina supracretacea*
25	*Bulimina arkadelphiana*	55	*Gaudryina bentonensis*	85	*Incertae sedis*
26	*Bulimina kickapooensis*	56	*Gaudryina bentonensis?*	86	*Lagena apiculata*
27	*Bulimina prolixa*	57	*Gaudryina boweni*	87	*Lagena hispida*
28	*Bulimina reussi*	58	*Gaudryina watersi*	88	*Lagena sulcata*
29	*Bulimina / Neobulimina sp.*	59	*Gaudryina sp.?*	89	*Laxostoma gemma*
30	*Caucasina vitrea*	60	*Globigerinelloides prairiehillensis*	90	*Lenticulina rotulata*

Key (continued)

91 *Lenticulina muensteri*
92 *Lenticulina sp. 2*
93 *Lenticulina sp.?*
94 *Lenticulina sp. / Pullenia sp.*
95 *Loxostoma plaita*
96 *Loxostoma sp.*
97 *Marginulina curvatura*
98 *Marginulina sp.*
99 *Neobulimina canadensis*
100 *Neobulimina canadensis beta*
101 *Neobulimina navarroana*
102 *Neobulimina sp.*
103 *Nodosaria sp.*
104 *Nodosaria affinis*
105 *Nodosaria aspera*
106 *Nodosaria proboscidea*
107 *Nuttallinella sp. / Osangularia sp.*
108 *Nuttallinella? disca*
109 *Nuttallinella sp. ?*
110 *Oolina obeliscata*
111 *Oolina sp.*
112 *Osangularia sp.*
113 *Osangularia navarroana*
114 *Palmula rugosa*
115 *Planulina kansasensis*
116 *Planulina sp.*
117 *Pleurostomella nitida*
118 *Psammosphaera sp. / Rotalia sp. ?*
119 *Psammosphaera caevigata*
120 *Pseudobolivina sp.?*
121 *Pseudoclavulina? meidamos*
122 *Pullenia sp.*
123 *Pullenia dakotensis*
124 *Pyrulina cylindroides*
125 *Quinqueloculina sp.*
126 *Quadrimorphina allomorphinoides*
127 *Ramulina muricatina*
128 *Ramulina sp. A*
129 *Robulus sp.*
130 *Robulus muensteri*
131 *Robulus spissocostatus*
132 *Robulus taylorensis*
133 *Rugoglobogerina rugosa*
134 *Saccammina complanata*
135 *Saccammina sp. ?*
136 *Saccammina / Oolina sp. ?*
137 *Saracenaria triangularis*
138 *Silicosigmoilina futabaensis*
139 *Silicosigmoilina sp.*
140 *Spiroplectammina laevis*
141 Sponge Spicules
142 *Stilostomella pseudoscripta*
143 *Stilostomella sp.*
144 *Tappanina costifera*
145 *Textularia sp. 1*
146 *Tritaxia sp. / Gaudryina stephensoni*
147 *Trochammina diagonis*
148 *Trochammina globosa*
149 *Trochammina ribstonensis*
150 *Trochammina sp. ?*
151 Unknown
152 *Valvuliveria centicula*
153 *Verneuilinoides perplexus*
154 *Verneuilinoides perplexus?*

Bibliography:

Bralower, T.J., Leckie, R.M., Sliter, W.V., and Thierstein, H.R. 1995. An Integrated Cretaceous Microfossil Biostratigraphy. in Berggren, W.A., Kent, D.V., Aubry, M.-P., and Hardenbol, J. (eds). Geochronology, Time Scales and Global Stratigraphic Correlation. SEPM Special Publication 54. p. 65-79.

Gill, J.R., and Cobban, W.A. 1965. Stratigraphy of the Pierre Shale, Valley City and Pembina Mountain Areas North Dakota. United States Geological Survey Professional Paper 392-A. 20p.

Hart, M.B., Bailey, H.W., Crittenden, S., Fletcher, B.N., Price, R.J., and Swiecicki, A. 1989. Cretaceous. in Jenkins, D.G., and Murray, J.W. (eds). Stratigraphical Atlas of Fossil Foraminifera, 2nd Edition. Ellis Horwood Limited, Chichester. pp. 273-371

Johnson, C.L. 1961. Microfauna of the Gregory Member of the Pierre Formation. Unpublished M.A. Thesis. State University of South Dakota. 185p.

Lange, A.U. 1962. Microfauna of the Verendrye Member of the Pierre Formation. Unpublished M.A. Thesis. State University of South Dakota. 135p.

Larson, D.W., Brinkman, D.B., and Bell, P.R. 2010. Faunal Assemblages from the Upper Horsehoe Canyon Formation, an Early Maastrichtian Cool-Climate Assemblage from Alberta, with Special Reference to the Albertosaurus sarcophagus bonebed. Canadian Journal of Earth Sciences. 47: 1159-1181.

Mello, J.F. 1969. Stratigraphy of the Upper Part of the Pierre Shale and Lower Part of the Fox Hills Sandstone (Cretaceous) North-Central South Dakota. United States Geological Survey Professional Paper 611. 117p.

Mello, J.F. 1971. Foraminifera from the Pierre Shale (Upper Cretaceous) at Red Bird, Wyoming. United States Geological Survey Professional Paper 393-C. 53p.

Petsch, B.C., 1942. The Medicine Butte Anticline. South Dakota Geological Survey Report of Investigations 45. 42p.

APPENDIX F Oil and Gas Shows Encountered During Project

Table F-1 Oil and Gas Shows – Preliminary

Location	Depth	Description
Tree Dam		
	202 ft.	Oil* show on coring table evidenced as a sheen. Appeared to come from 2 ft. thick interval in the core.
Presho #2		
	486ft.	Gas bubbles in mud pit were so vigorous that it turned into foam. Bubbles gone by 488ft. Oil sheen from 488-489ft. An obvious horizontal fracture in a shell bed may have been the source for the gas.
	491.5 ft.	Bubbles and foam -- all gone by 493ft.
	496 ft.	Bubbles -- gone by 498 ft.
	522 ft.	Bubbles -- no foam, disappeared by 524 ft.
	526 ft.	Bubbles -- no foam.
	532 ft.	Bubbles -- no foam.
	538 ft.	Small amount of an oil sheen with a few, small bubbles -- Very few compared with earlier shows.
	496 and 526 ft.	When cleaning the hole bubbles developed (repeat depths as seen the previous week).
	541 ft.	Bubbles -- hint of thin foam.
	543.5 ft.	A few bubbles.
	544-548 ft.	Bubbles.
	577-578 ft.	Small bubbles with audible effervescent.
	585.1 ft	Oil. After the core was out of the hole, more oil came up in the pit.
	599 ft.	Hint of oil also a very few/rare gas bubbles.
	604-609 ft.	Oil sheen in the mud pit with a few gas bubbles. Larger clumps of bubbles 608 ft. Bubbles were oil-coated, and persisted in the hand-held colander/screen.
	609- 614 ft.	Thin oil show from 609- 612ft. Gas was more frequent in the last 2 feet.
	614-619 ft.	Oil but no gas as coring began. Thicker oil with tiny gas bubbles at 617ft.
	619-620 ft.	Greater amounts of thicker oil with some bubbles.
	635 ft.	Bubbles and slight oil
	708 ft.	Gas bubbles
	722 ft.	Gas bubbles
*The term "Oil" in the these notes may or may not be oil in the proper sense - it was liquid and black, felt oily, and it was lighter in density, floating on top of the water. Even though light in density, at times it became thick and somewhat viscous. This material is awaiting analysis. Depths are based on drill rods in the hole and are, therefore, only approximate.		

APPENDIX G American Association of Petroleum Geologists Explorer Article -- 2015

AAPG EXPLORER
ROCKY MOUNTAIN ROUNDUP

Assessing Potential of the Rosebud Reservation

By LOUISE S. DURHAM, EXPLORER Correspondent

The upper Cretaceous Niobrara formation is widely known to be a highly commercial hydrocarbon producer, principally in Colorado and Wyoming.

Today, an intriguing program is afoot to assess the hydrocarbon potential of the Niobrara in south-central South Dakota.

Even though the formation is not ordinarily produced in this region, shows of natural gas are not unusual there. Some wells, in fact, are said to have produced gas for individual farms for as long as 20 years.

The current assessment program was initiated in 2012, when the American Indian Higher Education Consortium funded a cooperative education program between the Sinte Gleska University on the Rosebud Sioux Reservation in South Dakota and the South Dakota School of Mines and Technology (SDSM&T).

The aim was to involve Native American students in the energy resource evaluation process to provide educational opportunities that might result in energy exploration and production careers, according to AAPG member Daniel Soeder, research geologist at the U.S. Department of Energy's National Energy Technology Laboratory (NETL) in Morgantown, W.Va.

"Potential benefits to the Sicangu Lakota Oyate from the development of such a resource could include more jobs, economic development and an affordable energy source," Soeder said.

"The NETL has contributed in-kind geological and geochemical analyses and expertise to the project," he noted.

He explained that the objectives were to characterize the Niobrara in South Dakota in terms of stratigraphy, composition, depositional environments, reservoir properties, regional trends, structural features, potential productive horizons and areas.

Photo by Foster Sawyer, SDSM&T

Sarah Chadima (left) of the South Dakota DENR, and Mikal Bordeaux, a student at Sinte Gleska University, with a segment of Pierre Shale core recovered from a drill hole south of Presho, S.D.

Less Can Be More

The strategy, overall, was designed to use geological data and models to determine gas-in-place and EUR.

Soeder noted that there were no public drill cores available for study in the proximity of the reservation.

Not to worry.

The project participants undertook a trend analysis using Niobrara drill cores from Nebraska, Wyoming and western South Dakota, which were sampled at the USGS core library in Denver.

"The regional samples indicated that the Niobrara contains organic matter content as high as 6 percent, derived from Type II kerogen, and thermal maturity in the biogenic gas window," Soeder said.

"Porosity in the carbonate units may hold significant quantities of shallow gas," he added.

Meanwhile, the Department of Environment and Natural Resources Geological Survey in South Dakota is acquiring a new core from a well relatively close to the reservation. This might provide additional information given its proximal location.

Whatever the final conclusions of the study, the shallow depth of the Niobrara at Rosebud negates the possibility of production of the large volumes of gas desired by the commercial energy companies.

Less can be more, in some situations.

"The relatively inexpensive drilling costs and modest expected production may provide the tribe with a secure and economical energy supply," Soeder said, "suggesting a smaller-scale approach for unconventional gas development that could be applied elsewhere." E

SOEDER

AAPG member Daniel Soeder and some colleagues from the U.S. Department of Energy's National Energy Technology Laboratory will present the paper "Assessment of Hydrocarbon Potential in the Niobrara Formation, Rosebud Sioux Reservation, South Dakota," at the Unconventional Resources Technology Conference (URTeC) in San Antonio, July 20-22.

http://www.aapg.org/publications/news/explorer/emphasis/articleid/20404/assessing-potential-of-the-rosebud-reservation